

BeFo



STIFTELSEN BERGTEKNISK FORSKNING
ROCK ENGINEERING RESEARCH FOUNDATION

MATERIAL PROPERTIES OF BULK HYDROPHOBIC CONCRETE IN A NORDIC ENVIRONMENT

Patrick Rogers

MATERIAL PROPERTIES OF BULK HYDROPHOBIC CONCRETE IN A NORDIC ENVIRONMENT

**Egenskaper hos hydrofob betong i nordiskt
klimat**

Patrick Rogers

This report is a representation of the Licentiate Thesis in Civil and Architectural Engineering KTH Royal Institute of Technology Stockholm, "Material Properties of Bulk Hydrophobic Concrete in a Nordic Environment" © Patrick Rogers 978-91-8040-520-1 TRITA-ABE-DLT-231

This BeFo report is published with the permission of the author.

PREFACE

The main aim of this work has been to evaluate and measure the effectiveness of different potential hydrophobic admixtures in fresh concrete in order to increase the durability of the hardened product. This addition in the fresh concrete would negate the need to apply a protective coating in concrete structures subjected to harsh environments. The depth of penetration and the durability of the externally treated concrete surfaces would subsequently not be an issue.

This study showed that the interactions at the surface and further in at depths, where rebar is placed, can be significantly altered with the use of additives. Some of the bulk hydrophobic concretes investigated had sufficient reduction in water absorption and could potentially be applied in a Nordic infrastructural environment.

The research was conducted at RISE in cooperation with KTH and led by Jan Trägårdh and later Patrick Rogers. The research project was supported by a reference group Staffan Carlström (Swerock), Pär Fjellström (Besab), Behnam Dalili (Trafikverket), Iad Saleh (NCC) and BeFo (Per Tengborg).

The work has been co-financed with SBUF, Trafikverket, Energiforsk, Cementa, KTH and RISE.

Stockholm

Patrik Vidstrand

FÖRORD

Huvudsyftet med detta arbete har varit att utvärdera och mäta effektiviteten av olika potentiella hydrofoba tillsatser i färsk betong för att öka hållbarheten hos den härdade produkten. Dessa tillsatser i den färska betongen skulle kunna eliminera behovet av att applicera en skyddande beläggning i betongkonstruktioner som utsätts för tuffa miljöer. Inträngningsdjupet och hållbarheten hos de externt behandlade betongytorna skulle därefter inte vara ett problem.

Denna studie visade att interaktionerna på ytan och längre in på djupet, där armeringsjärn placeras, kan förändras avsevärt med användning av tillsatser. En del av de undersökta hydrofoba betongerna hade tillräcklig minskning av vattenabsorptionen och skulle potentiellt kunna appliceras i en nordisk infrastrukturmiljö.

Forskningen utfördes på RISE i samarbete med KTH och leddes av Jan Trägårdh och senare Patrick Rogers. Forskningsprojektet stöddes av en referensgrupp Staffan Carlström (Swerock), Pär Fjellström (Besab), Behnam Dalili (Trafikverket), Iad Saleh (NCC) och BeFo (Per Tengborg).

Arbetet har samfinansierats med SBUF, Trafikverket, Energiforsk, Cementa, KTH och RISE.

Stockholm

Patrik Vidstrand

SUMMARY

Concrete in its unaltered form allows the mass transfer of fluids into and out of its microstructure. These fluids can contain detrimental solutes which change the chemistry of the cement paste and/or the corrosion properties of the reinforcement bars, most noticeably hydrogen carbonates (HCO_3^-), oxygen (O_2) and chloride ions (Cl^-). Water and its solutions containing salts, mostly sodium chloride (NaCl), can also cause physical damage due to phase changes (freezing and thawing).

External application of hydrophobic agents onto the cement paste surface is a well-known method to alter the mass transfer at this interface. Bulk application of hydrophobic agents in ready mixed concrete is also a possible route but alters the entire cement paste.

This report presents relevant aspects concerning the use of bulk hydrophobic agents in concrete within a spectrum water to cement ratio (w/c) = 0.40-0.50. The main focus was on triacylglycerides (TAG) and alkyl alkoxysilanes (“silanes”) with application rates 1-3% based on cement weight.

Alterations to the compressive strengths have been observed and documented over a three-year period. The relative drop in mechanical strength is inversely proportional to w/c . The higher the addition rate, the lower the compressive strength. Chemical differences within the hydrophobic groupings (TAG or “silanes”) resulted in different outcomes. This was most noticeable in the water absorption, compressive strengths and chloride diffusion.

Freeze thaw testing did show noticeable differences, the use of “silanes” was detrimental in these tests even in deionised water. The exact mechanism is unknown, but thin section analysis shows a lack of air entrainer (even when added on the fresh concrete mix) and extensive cracking in the entire cement paste. The scaling in concrete with TAGs was smaller but needs further improving.

The main property intended to be enhanced with these agents was the ability to alter the mass transfer of water or solutions into the cement paste. Capillary suction and diffusion were examined. Increasing the w/c reduces the effectiveness of the hydrophobic agents to resist water uptake. This was seen in capillary suction and unidirectional chloride diffusion testing.

Processed TAGs were more effective in reducing chloride diffusion than the unprocessed chemical whereas, in some cases, the “silanes” actually increased the amount of chloride ions transferred into the cement paste. Only a slight positive effect can be seen at the lower inclusion rate (1%). Increasing the w/c reduces the resistance to chloride ion diffusion with the same dosage rate.

Keywords: Alkyl alkoxysilane, capillary suction, chloride ingress, concrete, diffusion hydrophobic agents, triacylglycerides

SAMMANFATTNING

Betong i sin oförändrade form tillåter masstransport av vätskor i och ur dess mikrostruktur. Dessa vätskor kan innehålla skadliga lösta ämnen som förändrar cementpastans kemi och/eller korrosionsegenskaperna hos armeringsjärnen, framför allt vätekarbonater (HCO_3^-), syre (O_2) och kloridjoner (Cl^-). Vatten och dess lösningar som innehåller salter, mestadels natriumklorider (NaCl), kan till och med orsaka fysisk skada på grund av fasförändringar (frysning och upptining).

Extern applicering av hydrofoba medel på cementpastans yta är en välkänd metod för att ändra masstransport genom denna gränssyta.

Bulkapplicering av hydrofoba medel i färdigblandad betong är också en möjlig väg, och resulterar i förändringar i hela cementpastan.

Denna rapport presenterar relevanta aspekter rörande användningen av bulk-hydrofoba medel i betong inom intervall av vattencementtal = 0,40-0,50 (vct). Huvudfokus låg på triacylglyceroler (TAG) och alkyl-alkoxisilaner ("silaner") med inblandning 1-3 % baserat på cementvikt.

Förändringar av tryckhållfasthet har observerats och dokumenterats under en treårsperiod. Den relativa reduktionen i mekanisk hållfasthet är omvänt proportionell mot vct. Ju högre tillsatsmängd i cementpastan desto lägre tryckhållfasthet. Kemiska skillnader inom de hydrofoba grupperna (TAG eller "silaner") resulterade i olika resultat. Detta var mest märkbart i vattenabsorption, tryckhållfasthet och kloriddiffusion.

Frysprovning visade märkbara skillnader, användningen av "silaner" var skadlig i dessa tester även i avjoniserat vatten. Den exakta mekanismen är okänd, men tunnslipsanalys visar på brist på luftporbildare (även om den tillsätts i stora mängder i den färska betongblandningen) och omfattande sprickbildning i hela cementpastan. Avskalningen i betong med TAG var mindre men behöver ytterligare förbättras.

De huvudsakliga egenskaperna avsedda med dessa medel var förmågan att förändra masstransport av vatten eller lösningar till cementpastan. Kapillärsugning och diffusion undersöktes. Att öka vct minskar effektiviteten hos de hydrofoba medlen för att motstå vattenupptagning. Detta sågs vid kapillärsugning och enkelriktad kloriddiffusionsprovning.

Raffinerade TAG:er var effektivare att minska kloriddiffusion än den oraffinerade, medan "silanerna" i vissa fall faktiskt ökade mängden kloridjoner som överfördes inne i cementpastan. Något positivt effekt kan ses vid den lägre inkluderingstillsatsen (1 %). Att öka vct minskar motståndet mot kloridjon diffusion.

Nyckelord: Alkyl-alkoxisilaner, betong, diffusion, hydrofoba ämnen, kapillärsugning, kloridinträngning, triacylglyceroler

NOMENCLATURE

Abbreviations

AE	air entrainer
ASTM	American Society for Testing and Materials
BY	attribution i.e. “by” creator
CC	creative commons
C.C.A.	commercial cleaning agent
CEM I	part of technical description of cement with Portland clinker content >94%
C.F.M	commercial filler metakaolin
C.F.UFL	commercial filler ultrafine limestone
C.H.A.	commercial hydrophobic agent
C.O.	corn oil
C-S-H	calcium silicate hydrate
EDL	electric double layer
GDP	gross domestic product
H.X.L	commercial corrosion inhibitor agent liquid
H.M.P.	commercial corrosion inhibitor agent powder
IBES	iso-butyltriethoxysilane
IR	infrared
IUPAC	International Union of Pure and Applied Chemistry
LA	low alkali
L.S.O.	linseed oil (RBD)
LWL	low water level
MH	moderate heat (cement)
N	normal strength development (cement)
NC	non commercial
ND	no derivative
NOMS	n-octyltrimethoxysilane
O.O.	olive oil (extra virgin)
OPC	Ordinary Portland cement
RBD	refined bleached deodorized
REF	reference (sample)
RH	relative humidity

R.S.O.	rapeseed oil (RBD)
SCM	supplementary cementitious materials
SP	superplasticizer
SR	sulphate resistant (cement)
S.S.O.	sesame oil (cold pressed)
TAG	triacylglyceride
w/c	water to cement ratio
WAT	water adding time
XRD	x-ray diffraction

Latin symbols

C_A	concentration of A	[mol/m ³]
D_{aadj}	diffusion chloride adjusted from 5 mm	[m ² /s]
D_{AB}	diffusion coefficient concrete	[m ² /s]
D_{NSS}	diffusion coefficient (non steady state)	[m ² /s]
D_{SS}	diffusion coefficient (steady state)	[m ² /s]
d_{max}	maximum aggregate size	[mm]
dx	change in distance x	[m]
f_c	compressive strength	[N/mm ²]
$J_{\text{Cl-}}$	flux (chloride ion)	[mol/m ² s ⁻¹]
M	Mol concentration	[mol]
p_c	pressure at sol. interface with capillary pore	[N/mm ²]
r	radius of capillary pore	[m]
W_{w24}	water absorption coefficient	[kg/m ² hr ^{1/2}]

Greek symbols

Δweight	change in weight	
$\sigma\text{-g}$	surface tension between liquid & gas	[Nm ⁻¹]
θ	contact angle	[°]

Subscript

24	Time 24 hrs
0-4 mm	Data disregarded from 0-4 mm from exposed surface
5 mm	Macro calculation shifted on x axis data at 5 mm → 0 mm

CONTENTS

PREFACE	i
FÖRORD	iii
SUMMARY	v
SAMMANFATTNING	vii
NOMENCLATURE	ix
1. INTRODUCTION	1
1.1. Cement clinker mineralogy and pore formation.....	1
1.2. Mass flow in cement paste.....	3
1.2.1. Negative impact of CO ₂ or Cl ⁻ in concrete.....	3
1.2.2. Mass flow mechanisms.....	4
1.2.3. Cost to society.....	6
1.3. Hydrophobic admixtures.....	7
1.3.1. Natural hydrophobic agents.....	7
1.3.2. Alkyl-silanes, alkyl siloxanes and alkyl alkoxy silanes.....	9
1.3.3. Calcium stearates and oleates (and other metallic soaps)....	10
1.4. Objectives.....	11
1.5. Limitations.....	11
2. SHORT LITERATURE SURVEY	13
3. METHODS	15
3.1. Water absorption.....	15
3.2. Compressive strength.....	16
3.3. Freeze thaw resistance.....	16
3.4. Chloride diffusion unidirectional.....	17
3.5. Capillary absorption of Cl ⁻ ; accelerated seasonal test.....	17
3.6. Isothermal calorimetry.....	19
3.7. Field station.....	21

4. RESULTS.....	27
4.1. Unidirectional water absorption in mortar and concrete.....	27
4.1.1. Water absorption in mortar discs.....	27
4.1.2. Water absorption in concrete	30
4.2. Compressive strength.....	34
4.2.1. Compressive strengths after 28 days - 3 years; concrete w/c = 0.40.....	35
4.2.2. General strength changes of all concretes with variable % hydrophobic additives at 28 days.....	36
4.3. Freeze thaw resistance of concrete.....	38
4.4. Unidirectional chloride diffusion.....	39
4.5. Capillary absorption of Cl ⁻ ; accelerated seasonal test.....	41
4.6. Isothermal calorimetry.....	42
4.6.1. w/c = 0.45 & 20 °C.....	42
4.6.2. w/c = 0.45 & 50 °C.....	43
4.7. Field station.....	47
5. DISCUSSION.....	49
5.1. Compressive strength.....	49
5.2. Water absorption from oven dry state (40°C).....	50
5.3. Freeze thaw resistance.....	51
5.4. Unidirectional chloride ion diffusion.....	51
5.5. Capillary absorption of Cl ⁻ , accelerated method.....	52
5.6. Iso thermal calorimetry.....	52
6. CONCLUSIONS.....	55
6.1. Water absorption.....	55
6.2. Compressive strength.....	55
6.3. Freeze thaw resistance.....	56
6.4 Chloride diffusion.....	56
6.5 Capillary absorption.....	56
6.6 Iso thermal calorimetry.....	56
6.7 Overall conclusion.....	57
7. REFERENCES.....	59
APPENDIX 1 - 6	

1. INTRODUCTION

Concrete is a heterogeneous material, consisting mainly of cement, water and aggregates of various sizes. The aggregates remain unchanged with time except in the case of alkali silica reaction [1]. The reaction products of cement and water though develop or break down with time and environment. Cement clinker and its additions, mainly gypsum, serve different functions in the reaction phases, i.e. when cement comes into contact with water.

1.1 Cement clinker mineralogy and pore formation

Cement clinker consists of four main clinker minerals: alite (Ca_3SiO_5), belite (Ca_2SiO_4), an aluminate ($\text{Ca}_3\text{Al}_2\text{O}_6$) and a ferrite ($\text{Ca}_2\text{AlFeO}_5$) phase [2]. Their reactions with water are exothermic but do not occur simultaneously but over a period of time. The cement fineness, clinker mineral makes up, availability of water, any additions to the cement and the surrounding temperature, determine when and how these reactions develop.

One can generalize that a typical cement clinker in a CEM I, as defined in [3], consists of 50-70 % alite, 15-30 % of belite, 5-10% aluminate phase and 5-15% ferrite phase. These are determined by the mass relationship between the raw materials entering the clinker manufacturing process, temperatures in the kiln and the rate of cooling post sintering. Additional information on other cement constituents such as alkalis can be found in works such as [2], [4], & [5].

The hydration of the alite and belite clinker phases is important in determining the structure of the cement paste. Physical properties such as compressive strength are directly attributed to the physical and chemical development of the hydrating minerals.

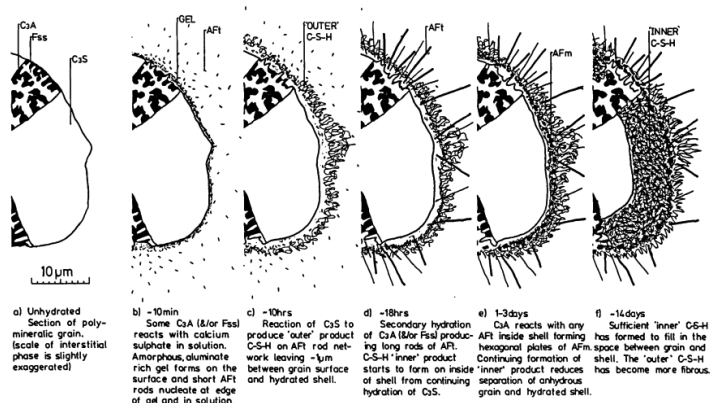


FIG. 6.1 Microstructural Development during the Hydration of Portland Cement

FIGURE 1.1. Microstructural Development during the Hydration of Portland Cement, Copyright [6] licensed under CC-BY-NC-ND 4.0.

At the beginning of the hydration stage, the cement paste is mainly large open pores up to 4000 μm , which, gradually reduce in size and volume %. The hydrating cement minerals alite and belite develop an amorphous calcium silicate hydrate commonly referred to as C-S-H. Referring to FIGURE 1.1., one can distinguish between inner and outer layers of C-S-H.

This continuing development of C-S-H over time (depending on availability of water and clinker minerals) leads to the formation of pores of various sizes, see FIGURE 1.2 below.

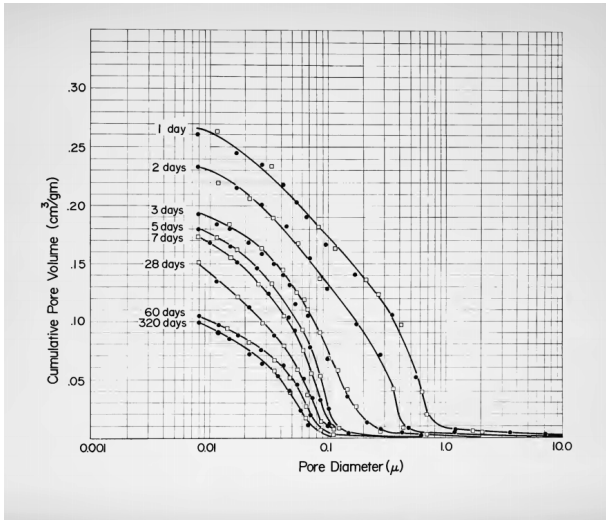


FIGURE 1.2. Pore size distribution and volume of cement paste with water:cement ratio = 0.4 hydrated at various ages [7].

These are mainly divided into capillary and gel pores. The capillary pores are formed by the space occupied by residual water (unreacted) whereas the gel pores are those formed due to the hydration and development of C-S-H. The material science of these C-S-H structures is complex due to the size of the pores, below 10 nm, and since these have water combined both between layers and adsorbed onto their structure(s).

The size ranges that are of interest to mass flow are within the size dimensions corresponding to the larger gel and capillary pores. The size of capillary pores can range due to how the cement paste/concrete was mixed (water cement ratio and admixtures), compacted and cured. In the literature, e.g., in [8], one finds references to capillary pores ranging in sizes between 5-50 nm up to 3-5 μm depending on these factors. There is more agreement on the size range of the gel pores being between 0.5 and 10 nm. The interface between the layers of C-S-H is small and only four water molecules can occupy this space, it is also fully saturated until the internal relative humidity reaches ca 11 % from saturation. The mass flow here is therefore not on the same scale as in capillary pores.

1.2 Mass flow in cement paste

Due to the size and volume of the pores, these are the primary route for mass flow in an uncracked, well compacted concrete. A considerable focus within the discipline of cement/concrete science is the inward mass transfer of CO₂ (or carbonate ion), O₂ (gaseous or absorbed in H₂O), sulphates and chlorides in the form of chloride ions. Outward mass flow normally consists of water in gas or liquid form, calcium salts, other alkalis present in the pore solution (fluid occupying the capillary pores), and even backward flow of chloride ions in a hypotonic solution, e.g., due to external washing or during rainfall.

1.2.1 Negative impact of CO₂ or Cl⁻ in concrete

The most sensitive components of reinforced concrete are the steel rebars and the cement paste. With sufficient concrete cover, the rebars are not directly exposed to the above-mentioned ions/compounds compared to the cement paste. The cement paste is directly exposed to the environment at the mass transfer interface i.e. the concrete's surface.

Inward movement of CO₂ and its reaction (as a dissolved hydrogen carbonate ion) with portlandite, i.e. carbonation, does reduce the pH of the pore solution. This in turn reduces the rebar steel's passivity and the corrosion products, if formed, will swell causing the concrete to spall which has a detrimental effect on the surrounding concrete.

The reason why chloride ions come in contact with concrete stems mainly from the use of deicing salts (calcium and sodium based), direct exposure to water borne chloride salts (oceans, and other chloride bearing bodies), or air borne salts driven by the wind over salt rich surfaces.

The influx of Cl⁻ has a negative effect on the cement paste but only if large quantities are transported into the cement paste pore system. According to [9], this would consist of an approx. 8 M chloride solution or > 6% Cl⁻/cement weight where the formation of expansive Friedel's salts in the form of Ca₂Al(OH)₆Cl·2H₂O (α) or (β) can develop [2]. The potential reaction i.e., swelling, would cause detrimental effects to the cement paste. These sequences occur provided the pH is high and that the original cement/binder mineralogy contained sufficient aluminate phases.

As with carbonation, the diffusion process within the cement paste, would allow sufficient chloride ions to reach further into the concrete and at a specified point in time to the rebar. At the rebar, the relatively thin pacified layer at the steel surface is disrupted due the ability of the Cl⁻ to penetrate this layer [10], [11], [12], [13] & [14]. This disruption causes the permeability of the layer to increase, enhancing the mass transfer of O₂ from the surroundings to the steel surface, hence increasing the potential for corrosion which was observed very early on after the first use of reinforced concrete [15], [16].

1.2.2. Mass flow mechanisms

Diffusion and capillary suction are the main mechanisms for chemical species to enter the cement paste pore system. As mentioned earlier, CO₂ and Cl⁻ are the two most important species due to their effect on the technical life of the steel rebar. The dominant mechanism depends on the pores' saturation state. These can differ at the interface between the concrete and the media in contact with the concrete, i.e., the pores exposed to the external surface compared with the pore system further away from the concrete's surface.

These interfaces can vary depending on location and environment, even time of day. For example, a concrete surface under the LWL (low water level) or submerged zone in maritime infrastructure will be in a constant state of saturation, whereas concrete in the same structure but in a location above this zone, i.e., the tidal zone and above, see FIGURE 1.3, states of saturation and “dry” conditions can prevail.

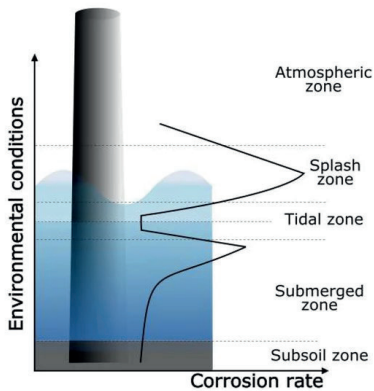


FIGURE 1.3. Zones of corrosion (y-axis) and relative corrosion rate (x axis) depending on the exposure zone. Copyright [17] Licensed under [CC-BY 4.0](https://creativecommons.org/licenses/by/4.0/)

Mass transfer mechanisms at the surface are different depending on the state of saturation within the pores. Diffusion processes are slow compared to capillary suction/action:

1.2.2.1 Diffusion:

Fick's first law can describe the flux of a solute in a solvent. A useful equation for species without any interaction with the surfaces they are permeating in is:

$$J_{Cl^-} = -D_{SS} \frac{dc_A}{dx} \quad \text{EQ 1.1}$$

Where J_{Cl^-} is the flux (chloride ions), D_{SS} is the diffusion coefficient (steady state), c_A is the concentration of A and x = distance between measured concentration and point of interest.

As chloride ions will react with aluminate phases present in the pore wall structure, the diffusion process becomes more complex and is in a non-steady state [18].

Applying a dimension for the binding of chlorides in a cement paste, Fick's second law can be rewritten to:

$$\left(\frac{\delta c}{\delta t}\right) = D_{NSS} \left(\frac{\delta^2 c}{dx^2}\right) \quad \text{Eq 1.2}$$

This equation is also a simplified version of reality as other phenomena are excluded such as electric potential field [19].

1.2.2.2. Capillary suction (action) potential

The potential for capillary flow can be describe as below in Eq 1.3,

$$p_c = \frac{\cos \theta \ 2\sigma_{l-g}}{r} \quad \text{Eq 1.3}$$

Where p_c is the sub pressure at the solution interface and capillary pore, σ_{l-g} is the surface tension between the solution and air (in unsaturated capillary pore), r is the pore radius, and θ is the contact angle between the capillary wall and solution's front [20].

Diffusion depends on a concentration difference (solute concentration), a distance, and a rate of diffusion (material property), see Eq 1.1. In a cement paste, this diffusion coefficient is directly related to the water to cement ratio (w/c) and its age, as this determines the pore size distribution and volume, see FIGURE 1.2. Lowering the w/c reduces the size of these pores and reduces D_{AB} . Typical ranges for D_{AB} in CEM I based concretes with w/c = 0.4 are ca $9.8 \pm 2.6 \times 10^{-12} \text{ m}^2/\text{s}$ [21].

Capillary suction/action is not dependent on a concentration barrier but mostly on the radius of the pores, the surface tension at the pore interface and the angle of the solution's front with the capillary pore, see Eq 1.3. A positive p_c value indicates no net movement of solution into the pore.

As capillary and gel pores are small in cement pastes, this type of mass flow can be very significant, it can even be assumed that the radii are not constant throughout the length of a capillary pore [20].

In a fully saturated capillary pore one can assume “pure” diffusion, even though absorption and desorption of species onto aluminates phases and effects of electric double layer (EDL) are likely [22, 23]. Lower saturation rates increase the amount of capillary flow suction/action but reduces as the pores fill.

At the surface of concrete, the effects of the varying relative humidity (RH) in air can be seen several millimeters into the surface, but research shows that at 15-20 mm into a surface exposed to Nordic external conditions, one can always expect high RH values in the cement paste pores [24]. Diffusion is therefore the majority mass transfer process from these depths and inwards.

One can therefore summarize that two mass transfer mechanisms can take place from the surface and to a depth equal to ca 15-20 mm (depending on the w/c of the concrete).

External infrastructural concrete can be assumed to have one dominant mechanism i.e. diffusion, from the aforementioned depth. The rebar is covered with a specific depth depending on the desired life span and/or environment of that structure and accordingly lie deeper than 20 mm from the concrete’s surface according to relevant national standards, e.g., [25].

1.2.3 Cost to society

The net effect of chloride and carbonate ion ingress into the cement paste to the level of the embedded rebar is a reduction of the steel rebar to resist corrosion. For this corrosion/damage to occur, there are certain conditions that need to be met, which are well reviewed in [13], e.g. the pH of the medium in direct contact with the rebar, the diffusion rate of O₂ and temperature to name but a few.

Corrosion of rebar in concrete is a large section of concrete science and the discussions are numerous [26-28]. Reinforced concrete is an important material for civil infrastructure, keeping its technical service life and even increasing it would be of interest to society as early or extensive repair work is expensive.

Work by [29] in the seventies showed that all forms of corrosion accounted to ca 3-4% GDP, this figure seems to have remained constant [30]. This would currently equate to ca US\$ 1.8-2.2 trillion per annum. It is estimated that US\$8.3 billion is annually spent by the Federal Highway agency on corrosion alone [31]. At present there is a ca US\$ 125 billion backlog of repair work on bridges in the USA according to [32].

These costs only include the direct costs and not those which can be associated with increased transportation costs or increased emissions to the environment.

Proper and timely maintenance could prevent some of the costs involved with infrastructure; one possible way is to hinder some of the prerequisites for corrosion. In concrete, this could be by reducing the w/c so that the Cl⁻ diffusion coefficient drops substantially or by altering the water absorption capability within the pores. This can be achieved with bulk or external application of hydrophobic chemicals.

1.3 Hydrophobic admixtures

The water molecule, H_2O , is covalently bonded and consists of two parts hydrogen and one-part oxygen. The higher affinity of the oxygen nucleus for the hydrogens' electrons, results in charge distribution whereby the hydrogen atom becomes more positive and vice versa for the oxygen atom. This is commonly referred to as dipolar. Ionic and polar molecules can easily dissolve in this fluid due to this charge arrangement. It is therefore advantageous for reinforced concrete structures to prevent ingress of water bound with potentially delirious ions, such as Cl^- , SO_4^{2-} or HCO_3^- , into the cement pore structure. This can be achieved with species that do not dissolve in water or hold no charge on its chemical structure. These are normally referred to as hydrophobic.

1.3.1. Natural hydrophobic agents

The use of hydrophobic admixtures or surface treatments onto building products and thereby reducing water absorption is not a new invention. In ancient Rome, the use of olive oil as a surface treatment and as an admixture was known as can be found in some excerpts from Vitruvius' "On Architecture" [33]. Here, though, one most note that ordinary Portland cement was not in existence for another ca 2000 years. The lime mortars used then were different in chemical composition and capillary pore structure compared to a modern cement paste/concrete. This allowed for external application of these oils to surfaces.

The main source of "vegetable" oils comes from the fruit of particular tree species such as olives (*Olea europaea*), oil palm fruit (*Elaeis guineensis*) or the seed or species such as rapeseed (*Brassica napus*). The chemical name for pure "vegetable" oils is triacylglycerol. The biosynthesis of which is the sequence of numerous enzymatic reactions including the final sequence whereby diacylglycerol undergoes acylation [34].

Other natural sources of hydrophobic admixtures used in mortars mentioned in literature include hog's lard, ghee, butter and other oils [35]. These are all esters of fatty acids with a trihydric alcohol (glycerol) backbone, see FIGURE 1.4 below.

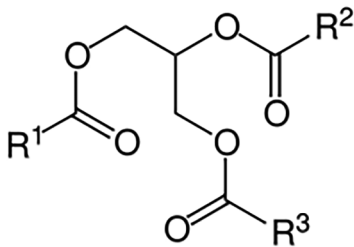


FIGURE 1.4. General structure of a triacylglycerol where R^{1-3} represents an array of fatty acids. Public Domain, [36].

The common denominator in these agents is the long-chained alkyl group, except ghee and butter which have a shorter fatty acid (butyric acid) consisting of four hydrocarbons.

These long chains of carbon and hydrogen atoms are the basis of immiscibility in water as the net electrical charge is evenly distributed over these extended chains. Creation of a net positive or negative region is therefore not existent. It is generally acknowledged, that hydrocarbon chains extending six or more alkyl groups in length are immiscible in water [37], [38]. Methanol and ethanol, CH_3OH & $\text{CH}_3\text{CH}_2\text{OH}$ respectively, are infinitely soluble in water, whereas octanol, $\text{CH}_3(\text{CH}_2)_6\text{CH}_2\text{OH}$, is only soluble to approx. $0.054 \text{ g}_{\text{octanol}}/100 \text{ g}_{\text{water}}$ [39]. Oleic acid, the main attached fatty acid of olive oil, $\text{C}_{18}\text{H}_{33}\text{O}_2$, is immiscible in water, see FIGURE 1.5 below.

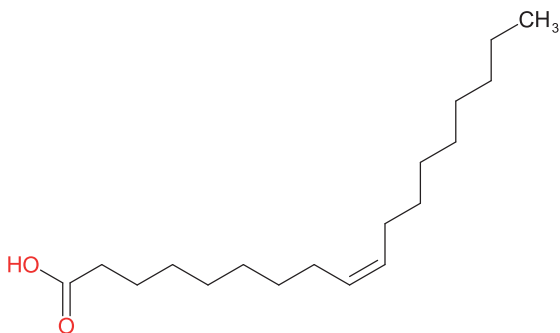


FIGURE 1.5. Simplified chemical structure of 9c-octadecenoic acid (oleic acid, a monounsaturated fatty acid)

The effect of adding triacylglycerol, e.g., olive oil, into a mortar compared to a reference mortar can be observed in FIGURE 1.6.



FIGURE 1.6. Plan view of cement mortar prisms 40 mm x 40 mm post destructive testing, $w/c = 0.50$ at 28 days

Left: REF without hydrophobic admixture; right: with hydrophobic admixture. Water drops applied to surface. The absorption of the water molecules into the pores of REF results in light dispersing effectively and the darker appearance of the surface. The water droplets are still stable and on the surface on the samples in the right photograph, roughly in the middle.

1.3.2. Alkyl-silanes, alkyl siloxanes and alkyl alkoxy-silanes

These are combination molecules based on silicon (inorganic) chemistry coupled with long-chained alkyl components (organic) which can be used in a basic environment, like in cement paste, and thereby adjust its surface properties. These, commonly referred to as “silane” products, are widely used in industry for a wide range of purposes.

The main production route for these organo silanes (Si-C) is based on the catalytic redistribution of tri chlorosilane and further alkoxylation to obtain a general $R_nSi(OR^1)_{4-n}$ structure, where $R = C_nH_{2n+1}$ and $R^1 =$ methyl, ethyl, pentyl etc. chain [40], [41].

Similarly, as with the triacylglycerols, it is the long-chained alkyl component that contributes to the hydrophobic nature of this chemistry once the process is complete, see FIGURE 1.7 and FIGURE 1.8.

In a basic environment, the “silane” molecule undergoes several processes (hydrolysis, condensation among molecules and then a condensation reaction with the substrate). This process is more thoroughly discussed in [42].

The Si-O-based part of the molecule attaches to a negatively charged hydroxide ion along the pores in the cement paste and a long alkyl chain protrudes outwards. Alkyl alkoxy-silanes are commonly used in the exterior application of concrete surfaces to produce a water repellent surface. These small (and as of yet unreacted) molecules can penetrate into the capillary pores provided the saturation levels are favourable. The hydrolysis of these alkyl alkoxy-silanes is dependent on the alkoxy component, the

larger the molecule, the slower the reaction. A detailed analysis of the extent of penetration and reaction can be found in [43].

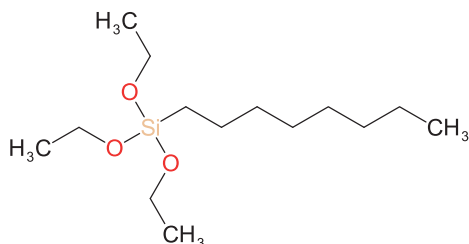


FIGURE 1.7. Simplified diagram of octyltriethoxysilane molecule. Note the eight-hydrocarbon chain, which is represented by the “zig-zag” line from the middle to the right of the figure, including the final “CH₃” originating from the “Si” atom, which will eventually give this structure its hydrophobic nature

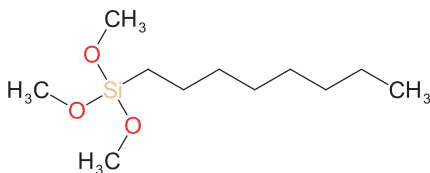


FIGURE 1.8. Simplified diagram of octyltrimethoxysilane. The distance from the other alkyl group to the silicon atom is shorter and increases the rate of reaction (hydrolysis) under the right conditions

Alkyls can generally be divided into acyclic- and cycloalkyls. Within hydrophobic applications, it is the acyclic alkyls that are of interest and have a general formula C_nH_{2n+1} and follow the nomenclature as set down by IUPAC [44]. The smallest member is methyl (C^1H_3).

1.3.3. Calcium stearates and oleates (and other metallic soaps)

Calcium stearates or oleates are metallic soaps produced on an industrial scale. Their uses are numerous, typically being applied as thickeners, lubricants and releasing agents, especially in the plastics industry.

The raw materials for this product are C_{18} fatty acids (cis-9-octadecenic or octadecenoic acid) and a metallic oxide, e.g. CaO. Its production route can either be via direct decomposition or direct reaction processes. The production of both raw materials consumes energy and the direct release of CO_2 during their processes [45].

Within building products, calcium stearate/oleate is of main interest as a damp proofing agent in a cementitious product as it has the characteristic long alkyl chain (C_{18}), see FIGURE 1.9, required to produce a hydrophobic effect. The product though is usually supplied in the powdered form and has a low solubility in water ca $0.04 \text{ g}/1000 \text{ g}_{\text{water}}$ @ 15°C .

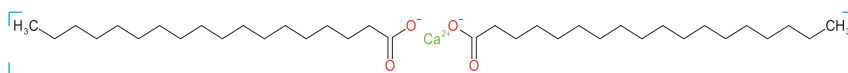


FIGURE 1.9. Simplified diagram of calcium stearate (Calcium octadecenoate)

1.4. Objectives

The work presented herein has two main objectives:

- 1) Design, mix and then measure relevant material properties applicable to bulk hydrophobic concrete. These properties should be relevant to Nordic environments and include properties such as water absorption, compressive strength, freeze-thaw resistance and chloride diffusion. Emphasis should be on concrete relevant to civil infrastructure.
- 2) Vary the water to cement ratio and the hydrophobic additives to determine if the concrete, as a whole, has a better performance than without the bulk hydrophobic additives.

Furthermore, it should be understood that this applies only to fresh concrete, as there are other established methods whereby hardened concrete surfaces can be modified to change its hydrophilic nature.

The objectives will need to be verified based on changes in material properties in the modified cement pastes / concretes. Normal concrete structures, e.g. bridges are designed for lifespans up to 120 years.

The inclusion of bulk hydrophobic additives in to concrete is supposed to reduce the mass flow of detrimental ions into the capillary pore structure, does this increase the lifespan of the concrete structure?.

1.5 Limitations

Concrete science benefits from the past, as specimens, e.g. old bridges, have been exposed to different scenarios over a long period of time. These concretes were designed and manufactured with cements that most likely do not exist anymore. The use of additives, e.g. superplasticizers, retarders etc., was not as prevalent. We are at a point in time where focus on climate impact has changed the scope of available cement types

in Sweden. The mortars/concretes in this thesis have only used CEM I 42,5 N products from a cement plant that no longer produces clinker. Natural aggregates have also only been exclusively used, which is also on a downward trend due to its impact on groundwater. The use of new cement replacement materials and crushed aggregates is not taken into consideration in this thesis. Limitations to the scope of raw materials in this thesis could be used as reference data as most would have access to local natural aggregates and a CEM I cement. Vast differences in access to supplementary cementitious materials (SCM) and crushed or alternative aggregates complicates comparisons.

2. SHORT LITERATURE SURVEY

As briefly mentioned in the introduction, creating hydrophobic surfaces on building materials was already carried out in the ancient Roman times. Their binder material, mainly slaked lime, was of course different to the infrastructural building materials used today, which is nearly entirely based on cement (OPC and compositions thereof). The changing geometry of structures from arches to beams and slabs, with their need for rebars to increase tensional performance, has made them more vulnerable.

There are numerous studies into the effect of hydrophobic agents in cementitious products, e.g. [46-48] to mention just a few.

All additions based on TAGs caused a reduction in compressive strength. Most studies though are limited to only a few percentages, usually 1-2%, based on cement weight. Very few studies investigate the effect of bulk hydrophobic agents in concrete, e.g. [49], here, the effect of a TAG (rapeseed oil) was compared to a free fatty acid (stearic). Other TAGs in mortars and concrete have been studied and reflect the regional flora e.g., castor oil (*Ricinus communis*) in [50]. Here though the structure of the fatty acid, 12-hydroxy-9-cis-octadecenoic acid, is more polar than those in e.g., olive oil or rapeseed oil.

To the author's best knowledge, not many studies have focused on freeze thaw resistance of bulk hydrophobic concrete, a study in the 60's [51] looked at the inclusion of "silicones" into and onto concrete and concluded that neither of them were beneficial to the freeze thaw resistance compared to the reference.

A more recent study [52] showed the inclusion of a silane "oil in water" mix, up to 4%, could enhance the freeze thaw resistance of a concrete, including a reduction in chloride diffusion.

Differences in effectiveness between surface and bulk hydrophobic cement pastes were evaluated in [53] showing surface treatment to be of limited use in hindering inward mass transfer of a strong sodium chloride solutions. This though was not observed in the bulk application.

It has been observed that TAGs can be more effective than alkyl alkoxysilane in reducing water absorption [54].

Other benefits in terms of corrosion resistance of reinforced concrete in the presence of induced cracks have been studied [55] and shown that the inclusion of an alkyl-triethoxysilane increased the diffusion of oxygen in the cracked region, increasing the rate of corrosion when permanently exposed to a sodium chloride solution. This though changes if a wet and dry cycle is introduced as part of the sodium chloride solution exposure [53], whereby the corrosion process in the bulk hydrophobic specimen was found to be less than the corresponding one of the references.

3. METHODS

This chapter will provide an account of the methods employed during the experimental work.

3.1. Water absorption

The water absorption coefficient, W_{w24} , of mortars and concrete was determined using the method described in ISO 15148:2002 [56]. The weight increases of three $\text{\O}100$ mm slices per subset (mix) were measured over time until the rate of water absorption plateaued. Initial testing involved slices approx. 20 mm in height, but for concretes this was increased to approx. 80 mm, see FIGURE 3.1. All specimens were preconditioned in a forced convection oven at 40°C & ca 11 % RH. The time to begin testing varied due the difference in w/c and the height of the specimens (dominating factor). The longest duration was 6.5 months.

The initial testing was carried out on 20 mm slices of the mortar mixes (w/c) = 0.50 and would have featured in the results of [77] but were not ready at the point of submission. Subsequent testing was on concrete at w/c = 0.40, 0.45 and 0.50. Within the w/c = 0.40 testing, concretes with air entrainer were also examined.



FIGURE 3.1. Water absorption test of $\text{\O}100$ mm & 80 mm thick concrete specimens; w/c = 0.50. Three specimens per recipe. Specimens placed on a textile-based material which itself lies on a plastic raised bed filled with water. Sawn concrete exposed to water (bottom) and the ambient air (top). A 3 mm thick neoprene layer was applied to the sides of the cylinders.

3.2. Compressive strength

The measurement of compressive strength is a fundamental property for material science research and in particular within concrete/cement-based sciences. An important input in determining the outcome of the testing is the water to cement ratio (w/c) of the cementitious mix. The lower the w/c, the higher the compressive strength. A higher w/c leads to more capillary pores that do not contribute to the structural loading capacity. Any change to the structural integrity of the concrete can be empirically determined by comparing the results within the same subgroup, e.g. w/c and time.

The time interval between casting and testing is also an important parameter. Different cement clinker minerals, mainly alite and belite, have different reaction rates. A standard testing interval is 28 days after casting. Additional testing was carried out to determine the development of strength over time and includes testing after one and three years.

In Europe, the testing of concrete compressive strength is determined by EN 12390-3:2019 [57]. All concrete specimens were cast into 100 mm sided cube moulds (without demoulding oil) as described in SS-EN 12390-1:2021 [58] and cured in a climate room $20\text{ °C} \pm 2\text{ °C}$ and $98\% \pm 2\%$ RH after demoulding.

Mortars were cast into standard 160 mm x 40 mm x 40 mm moulds (without demoulding oil) and tested for compressive strength as described in SS-EN 196-1:2016 [59]. These were also cured in the same climate room as mentioned above.

3.3. Freeze thaw resistance

Freeze thaw resistance is an important material property for concrete used in external civil engineering structures in cold climates. This is particularly applicable to regions where the temperature fluctuates above and below -5 °C many times per season. There are two methods in Sweden that can be used depending on the region of application. A concrete surface is exposed to either to a layer of deionised water or a 3 wt% NaCl solution for 56 temperature cycles as described in [60]. This method is very similar to that the European method in [61]. Results under 1.00 kg/m^2 after 56 cycles are deemed “acceptable”. A concrete recipe usually used in bridge construction was modified to include bulk hydrophobic agents and is described further in [78]. Some of the concretes were retested and samples were cored from the presented concrete from [78] and tested for compression strength.

3.4. Chloride diffusion unidirectional

An important aspect of a reinforced concrete reaching its technical life span is that the rebars do not corrode. Ingress of Cl^- (and/or CO_2) into the cement paste are an important indicator of the remaining technical life of the concrete. Measuring how well a cement paste hinders the mass transfer into the concrete is a tool to predict and plan for technical life spans. As with compressive strengths, w/c plays a pivotal role in the diffusion resistance of cement pastes. The maturity of the cement paste is also a factor as the cement paste pores become more refined with time i.e., diffusion takes longer.

These tests take a long time to complete and accelerated methods exist (35 days of exposure) such as ASTM C1543, [62], and similarly NT BUILD 443, [63]. The sodium chloride content is rather high (165 g/l) ca 2.8 M. It was decided to use SS-EN 12390-11:2015, [64] as the solution concentration is 0.5 M but the testing duration is 91 days.

3.5. Capillary absorption of Cl^- ; accelerated seasonal test

This method describes a short test to evaluate the effectiveness of bulk hydrophobic agents in concrete to capillary action of a 3% NaCl salt spray. The concrete was exposed to four artificial seasons over a period of one week, during which the temperature and RH % fluctuates. This was then repeated an additional seven times.

Four cylindrical specimens ($\text{Ø} = 100 \text{ mm}$) from the w/c = 0.50 series, see FIGURE 3.2, were preconditioned at $20 \text{ °C} \pm 2 \text{ °C}$ & $85 \pm 2\% \text{RH}$ until the weight stabilizes to $\Delta \text{weight} < 0.1\%$. The specimens were then sealed with a self-adhesive 3 mm thick neoprene layer exposing only one surface, i.e. the sawn surface, see FIGURE 3.2.

These were placed back in the climate box (85 % RH) until testing and reweighed.

The aim with the NaCl solution spray was to apply a realistic amount of NaCl per unit area and “year” whilst also providing ease of execution. 30 g NaCl/m² in total was applied each “winter” and correlates to approx. 10% of the findings of [65] & [66]. Pre trials showed that excessive amounts of the NaCl solution, equivalent to the amounts found in the author’s works, would accumulate in the plastic lining and not contribute to the findings.

The four concrete specimens were taken from the “autumn” climate box and placed in a small plastic container with an area of 0.1 m². The exposed area was horizontally aligned with the container and a plastic underlay allowed any excess solution to run off the specimen. The rig was transferred to the “winter” room and allowed to cool to ambient temperature which was measured with an IR thermometer. Thereafter 15 g NaCl/m² equivalent was sprayed over the rig at a vertical distance of 0.5 m. Four hours later the same procedure was repeated. The samples were then removed ca three hours later and placed in the “spring” climate box. The specimens were weighed at each point and were transferred from one “season” to the next according to TABLE 3.1. The whole

procedure was repeated 8 times (the surfaces were never cleaned at any stage). The specimens were then dry ground in millimeter steps and the chloride contents analyzed according to [67].

TABLE 3.1. Artificial year for capillary action comparison in concrete.

Season	Temp [°C]	RH [%]	Duration [days]
Winter	5 ± 1	50-60	0.5
Spring	20 ± 2	75 ± 3	1.5
Summer	40 ± 2	10-20	2.0
Autumn	20 ± 2	85 ± 3	3.0



FIGURE 3.2. Four sawn concrete cylinders ($\varnothing = 100$ mm height = 85 mm). Neoprene layer applied to all surface except the top.

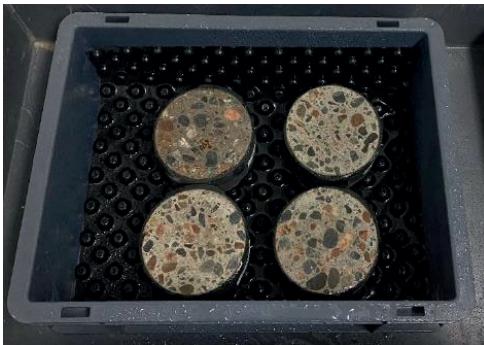


FIGURE 3.3. Concrete specimens after spray application placed in plastic container 37.5 cm x 26.5 cm. REF 0.50 top left (darkest surface); top right n-octyl 3%; bottom left O.O. 3%; bottom right R.S.O 3%.

3.6. Isothermal calorimetry

The inclusion of hydrophobic admixtures should not alter the hydration of alite or belite in a negative way i.e. neither retard, accelerate nor reduce the hydration rate. The analysis of the heat liberated in a cement paste, e.g. see FIGURE 3.4, during the first 72 hours gives a good indication as to what, if anything, the hydrophobic admixtures do to the hydration chemistry.

Isothermal calorimetry measures the energy required (removal or addition) to keep a temperature constant in a well-insulated chamber, e.g. 20 °C. The hydration of cement clinker minerals is exothermic, so the heat energy removed over time is recorded and compared against active sample weight (i.e. cement). The equipment used was an eight channel TAM Air placed in a temperature-controlled room at 20 °C ±2 °C.

The hydrolysis reaction of alkyl alkoxysilane in a basic environment is endothermic. Triacylglycerides can saponify at lower and higher temperatures in a basic environment according to [68] but in order for the saponification to occur at lower temperatures a catalyst is required. Free fatty acids are known to act as a catalyst, which would be present in the mechanically processed triacylglyceride based on *Olea europae* but not in the heavily processed triacylglycerides from *Brassica napus*. The levels of free fatty acids are close to zero due to an alkali cleaning process (neutralization) [69].

The reaction product(s) from saponification of triacylglycerides are fatty acid(s) and either diacylglyceride, monoacylglyceride or glycerol depending on the extent of reaction [38]. All the non-fatty acids are polar molecules.

Measuring the change in heat released with the addition of glycerol on cement hydration will provide a characteristic heat pattern increasing the C₃A and C₄AF minerals [70]. At relatively low levels, 0.3-1.5%, it can even liberate more heat during the induction phase according to [71]. Comparing this with the heat signal acquired during the cement hydration with triacylglycerides will indicate whether saponification occurs in the basic conditions and temperatures during hydration.

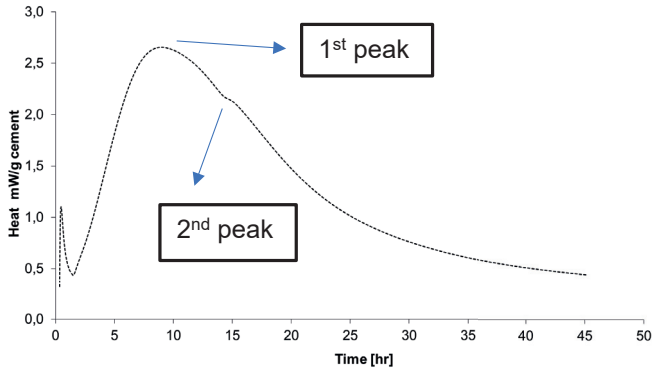


FIGURE 3.4. Typical cement heat generation of ordinary Portland cement, with peak after approx. 10 hours whilst kept at 20°C. Cement is of the “moderate heat” type i.e. higher belite content.

The cement used in these experiments was a bagged CEM I 42,5 N LA/MH/SR3, w/c=0.45. The total weight of each batch was 1450 g and mixed in a suitable mixer as mentioned in [59] for 5 minutes. Syringes filled with the admixtures, see TABLE 3.2 below for details, and were prepared in advance so that the combination of these equated to a 1%, 2%, 3% and 5% addition (based on cement weight). As the amount of cement paste is rather small compared to the bulk (ca 0.5%) the effect of dilution was deemed negligible. After a sample was extracted using a clean syringe, the next addition level was added into the cement paste and mixed thoroughly for two minutes. The sampling was repeated until the entire range for the set had been added.

TABLE 3.2. Iso thermal calorimetry matrix.

Specimen	Temp	Temp	Addition
	[°C]	[°C]	[%]
REF (w/c = 0.45)	20	50	0
REF + triacylglyceride (<i>Olea europaea</i>)	20	50	1, 2, 3 & 5
REF + triacylglyceride (<i>Brassica napus</i>)	20	50	1, 2, 3 & 5
REF + n-octyltriethoxysilane	20	50	1, 2, 3 & 5
REF + propane 1,2,3 triol (glycerol)	20	50	0.1*,0.2* & 0.3*

*These values equate to the stoichiometric equation from the saponification of 1, 2 & 3% triacylglyceride. Due to the retarding effect of propane 1,2,3 triol at higher additions, the 0.5% step was omitted.

The weight of the active samples was ca $7.000 \text{ g} \pm 0.100 \text{ g}$ and was filled into plastic ampoules, see FIGURE 3.5. An inert co sample (water) was placed in the pair chamber. The temperature of the room was kept constant.



FIGURE 3.5. Plastic ampoules used for iso thermal calorimetry, ca 7.00 g sample per ampoule.

The data are analyzed based on the heat removed, the time from the addition of water (WAT) and the known weight of the active ingredient in the sample.

3.7. Field station

A ca 10 m bridge edge beam section in Stockholm was made available for long term testing of concrete in stainless steel cages, see FIGURE 3.6-FIGURE 3.9. The address is Magelugnsvägen on road 271, the exact location is $59^{\circ}16'23'' \text{ N } 18^{\circ}00'47'' \text{ E}$ and is also captured via popular cartographic software in [72].

The location was chosen due to its proximity to CBI/RISE laboratories, it is operated by Stockholm municipality, is on the outer lane and has no obstructions between the vehicular traffic and the concrete surface (except for the safety cage around the specimens). This stretch also has a high-speed limit (70 km/h) increasing the potential spray distance of passing traffic.

The aim of the field station is to expose the concretes to real conditions and compare the chloride ingress in the bulk hydrophobic concretes with the reference concretes.

These concretes were installed in stages, see recipes in TABLE 3.3-3.5. The first three cages were installed in January 2018. The two others are used in another project [73]. An additional testing cage was installed in 2019 to accommodate 12 additional concrete recipes.

TABLE 3.3. Recipes for initial field station installed in January 2018.

	REF (0.40) w/o air entrainer	REF 2 (0.40) with air entrainer	Concrete modified with bulk hydrophobic agent
	[kg/m ³]	[kg/m ³]	[kg/m ³]
CEM I 42.5 LA/SR3/MH	430.0	430.0	430.0
Water	172.0	172.0	172.0
Natural Aggregates 0-8 mm	865.1	865.1	865.1
Natural Aggregates 8-16 mm	865.0	865.1	828.8
Air Entrainer *	0.0	0.17	0.0
Superplasticizer**	0.0	2.0	0.0
Bulk Hydrophobic Agent	0.0	0.0	12.9

The bulk hydrophobic agents' density differences were compensated with volume changes in natural aggregates if required.

TABLE 3.4 Explanation of bulk hydrophobic agents.

Bulk Hydrophobic Agents
TAG* <i>Olea europaea</i> (Mechanical Extraction)
TAG <i>Brassica napus</i> (RBD)
Organofunctional silane based admixture
Octyltriethoxysilane based admixture

*TAG = triacylglyceride ("vegetable" oil)

TABLE 3.5. Recipes for field station installed in 2019.

REF (0.40) *Crushed aggregates 0-8 mm	no AE or SP
REF (0.40)	no AE or SP
REF (0.40)	AE + SP
C.H.A 2 (0.40) 3%	no AE or SP
C.H.A 2 (0.40) recommended dosage	no AE
C.H.A 3 _{powder} (0.40) 3%*	no AE or SP
C.H.A 3 _{liquid} (0.40) 3%	no AE or SP
TAG(0.40) <i>Olea europaea</i> (Mechanical Extraction) 3%	no AE or SP

TAG(0.40) <i>Olea europaea</i> (Mechanical Extraction) 3%	AE
TAG (0.40) <i>Brassica napus</i> (RBD) 3%	AE
TAG (0.40) <i>Brassica napus</i> (RBD) 3%	no AE + SP
TAG (0.40) <i>Brassica napus</i> (RBD) 3%	no AE or SP

All recipes based on same as REF (0.40) in TABLE 3.3.

AE= Air Entrainer

SP= Superplasticizer

C.H.A. 2= Commercial corrosion inhibitor based on octyltriethoxysilane and isotridecanol (ethoxylated).

C.H.A. 3 = Commercial hydrophobic agent and corrosion inhibitor (powder and liquid form), proprietary agent based on an alkali salt of a dioic acid with branched hydrocarbon.



FIGURE 3.6. The initial field station installed 11th January 2018. The concretes are 100 mm sided with neoprene outer shell, exposing only the sawn surface. Concrete age at time of exposure ca 3 months.



FIGURE 3.7. Autumn check of the specimens, the area between the raised edge beam and asphalt is rarely dry.



FIGURE 3.8. View looking back to Älvsjö, double lane going in both directions with a concrete barrier separating the traffic flow. Water and debris accumulate in this vicinity.



FIGURE 3.9. Driving past the field station 8th January 2022. Snow has accumulated on level with the top of the safety cages, see the blue arrows. The lane between the car and the edge beam, i.e. where the specimens are fixed, is a merging lane see [74].

4. RESULTS

Within this chapter summaries of the more important findings are presented. Additional information or similar findings within a subset will be referred to in the relevant appendix.

4.1. Unidirectional water absorption in mortar and concrete

The results within this section are divided up in two, mortar and concrete. Within the concrete results there is a further subdivision based on water to cement ratio (w/c).

4.1.1. Water absorption in mortar discs

The results from the water absorption tests are presented in FIGURE 4.1. & FIGURE 4.2. Each point represents the average weight change of three Ø100 mm discs (ca 20 mm thick). The two diagrams are divided into mortars with triacylglycerides (TAG) in FIGURE 4.1 and mortars with commercial admixtures in FIGURE 4.2 The comparative coefficient of water absorption, W_{w24} , is presented in TABLES 4.2 and 4.3 for all results. W_{w24} is calculated using the change in mass from $t = 0$ h (initial exposure to water) to 24 h (continuous exposure) divided by the square root of time in hours.

TABLE 4.1. Abbreviations of the additives used in the experiments (w/c = 0.40, 0.45 and partly in 0.50)

Hydrophobic agent/admixture	Description	Other general terminology
O.O.	Olive Oil (extra virgin, cold pressed, food grade)	TAG (unprocessed)
C.O.	Corn / Maize Oil (RBD, food grade)	TAG
L.S.O.	Linseed Oil (RBD; food grade)	TAG
S.S.O.	Sesame Oil (cold pressed, food grade)	TAG
R.S.O.	Rape Seed Oil (RBD; food grade)	TAG (processed)
C.C.A.	Commercial Cleaning Agent; fatty acid potassium soap	
H.X.L (liquid) H.M.P (powder)	Commercial hydrophobic agent and corrosion inhibitor (powder and liquid form) proprietary agent based on an alkali salt of dioic acid with branched hydrocarbons	
C.H.A. 1	Commercial water repellent/hydrophobic agent (60 % alkyl silane based)	
C.H.A. 2	Commercial corrosion inhibitor based on octyl triethoxy silane and isotridecanol (ethoxylated)	

Below, in FIGURE 4.1, are the water absorption results from mixing 3% TAG into the mortar mixes.

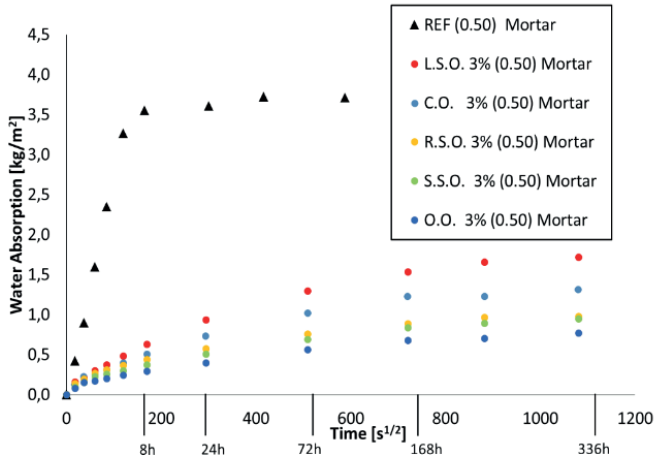


FIGURE 4.1. Water absorption results from mortar $w/c = 0.50$; 3% addition of TAG. Span over two weeks. The arrangement of the legend reflects the rate of water absorption from most (top) to least (bottom). The x-axis has two scales to ease interpretation of the time scale.

Here, one observes the rapid absorption of water in the reference sample, see the black triangular data points, REF (0.50). It remains at a constant level after eight hours. The saturation point is affected by the thickness of the disc (ca 20-22 mm) and loss of vapour to air. Distinctions can be seen with different chemical structures of triacylglycerides (TAGs). Within the TAG subset, the addition of olive oil (O.O.) resulted in the least amount of water absorption and linseed oil (L.S.O) the most.

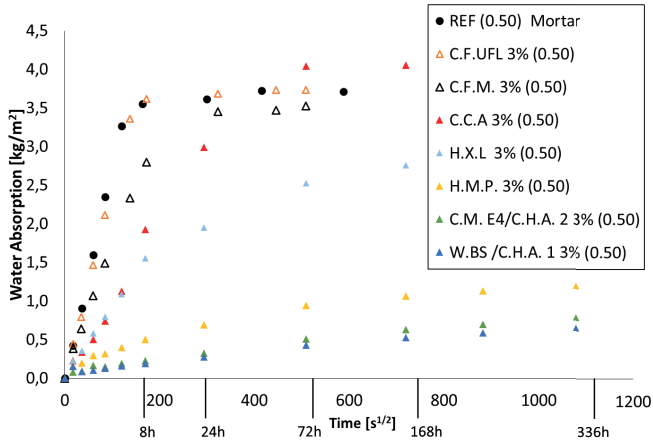


FIGURE 4.2. Water absorption results from mortar $w/c = 0.50$; 3% addition of commercial products. Span over two weeks.

The span of results is more varied in FIGURE 4.2 compared to FIGURE 4.1. The observations can be divided into three regions. Firstly, the addition of fillers, e.g., limestone, C.F.UFL 3% (0.50), had no appreciable water absorption difference compared to the reference (see data points with black circles and hollow orange triangles). Metakaolin, C.F.M. 3% (0.50) reduced the initial slope, see black hollow triangles. Two commercial products, C.C.A 3% (0.50) and H.X.L. 3% (0.50) had similar weight increases from zero to six hours but then diverged, see blue and red triangles. Of note are the noticeable differences in the water absorption results represented by the blue and yellow triangles, i.e. H.X.L 3% (0.50) and H.M.P 3% (0.50), which are essentially the same chemical except “L” = liquid and “P” = powder.

Among the tested commercial products, it was the silicon and hydrocarbon-based products i.e., C.M. E4/C.H.A.2 3% (0.50) and W.BS/C.H.A. 1 3% (0.50) that reduced water absorption the most. A further summary of W_{w24} can be seen in TABLES 4.1 and 4.2.

TABLE 4.2. Water absorption coefficient results, W_{w24} , mortars with inclusion of triacylglycerides (TAG) commonly referred to as “vegetable” oils.

Mortar recipe	W_{w24} [kg/m ² hr ^{1/2}]	Reduction compared to REF [%]
REF (0.50)*	1.63	
O.O. 3% (0.50)	0.08	-95
S.S.O. 3% (0.50)	0.10	-94
R.S.O. 3% (0.50)	0.12	-93
C.O. 3% (0.50)	0.15	-91
L.S.O. 3% (0.50)	0.19	-88

*Due to the rapid water absorption of the cement paste, the results were based on the period where the mass increase was in a steady state of increase, i.e. between the point from $t=0$ to 6 hours.

TABLE 4.3. Water absorption coefficient results, W_{w24} , mortars with inclusion of commercial products.

Mortar recipe	W_{w24} [kg/m ² hr ^{1/2}]	Reduction compared to REF [%]
REF (0.50)	1.63	
W.BS / C.H.A 1 3% (0.50)	0.06	-96
C.M. E4 / C.H.A 2 3% (0.50)	0.07	-96
H.M.P 3%(0.50)	0.14	-91
H.X.L 3%(0.50)	0.40	-76
C.C.A. 3%(0.50)	0.61	-63
C.F.M. 3%(0.50)*	0.97	-40
C.F.UFL 3%(0.50)*	1.46	-10

*Due to the rapid water absorption of the cement paste, the results were based on the period where the mass increase was in a steady state of increase, i.e. between the point from $t=0$ to 6 hours.

4.1.2. Water absorption in concrete

This subsection shows the water absorption of concrete discs, the recipe can be seen in [78]. The w/c ratio is 0.40 without the use of air entrainer. The purpose of this concrete was to design and test a concrete which could be suitable for Nordic infrastructural projects. The results from Section 4.1.1 were used as a screening process whereby the most effective hydrophobic chemicals were mixed into concrete.

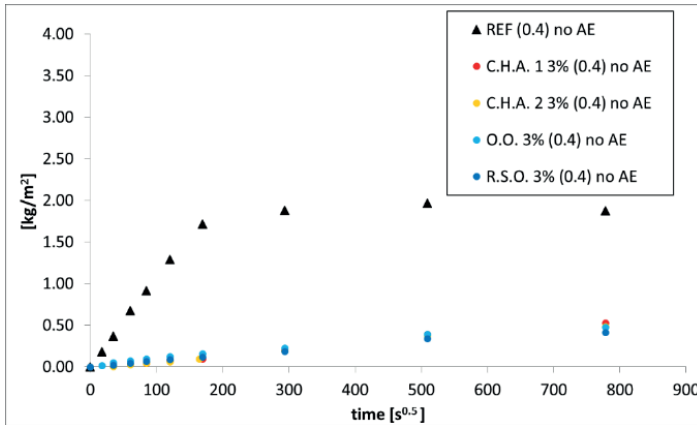
4.1.2.1 Water absorption in concrete $w/c = 0.40$ 

FIGURE 4.3. Water absorption (one week) concrete $w/c = 0.40$ without air entrainer. Disc: $\varnothing 100$ mm, thickness ca 20 mm. “w/o AE” = without air entrainer.

A similar pattern emerges as seen in FIGURES 4.1 and 4.2, whereby the hydrophobic admixtures reduce the rate of water absorption within the cement paste and the cement paste and aggregate interface. A summary of the water absorption coefficients is presented in TABLE 4.4. The graphical results from the concretes with air entrainer can be found in APPENDIX 3.

Interestingly, the use of this particular air entrainer can increase the water absorption coefficient, see TABLE 4.5.

TABLE 4.4. Water absorption coefficient results, W_{w24} , from concrete $w/c = 0.40$ without air entrainer (w/o AE)

Concrete recipe	W_{w24} [kg/m ² hr ^{1/2}]	Reduction of W_{w24} compared to REF [%]
REF (0.40) w/o AE	0.607	
R.S.O. 3% (0.40) w/o AE	0.069	-88
O.O. 3% (0.40) w/o AE	0.046	-92
C.H.A. 1 3% (0.40) w/o AE	0.040	-93
C.H.A. 2 3% (0.40) w/o AE	0.039	-93

TABLE 4.5. Water absorption coefficient results, W_{w24} , from concrete $w/c = 0.40$ with air entrainer (AE)

Concrete recipe	W_{w24} [kg/m ² hr ^{1/2}]	Change compared w/o AE sample [%]
REF (0.40) 7.2%	0.565	-7
R.S.O. 3% (0.40) 2.5%	0.052	-25
R.S.O. 3% (0.40) 6.2%	0.059	-15
O.O. 3% (0.40) 2.5%	0.052	+13
O.O. 3% (0.40) 5.4%	0.056	+21
C.H.A. 1 3% (0.40) 2.5%	0.043	+7
C.H.A. 2 3% (0.40) 4.9%	0.051	+30

The percentage figure after (0.40) indicates the air content measured in the fresh concrete.

4.1.2.2. Water absorption in concrete $w/c = 0.45$

The results from the previous section were used in a self-contained proposal to produce a freeze thaw resistant concrete for Nordic conditions according to exposure class XD3, which included even a substantial reduction in water absorption. Following the results, which can be referenced in Section 4.3 and [78], the scope was expanded to include a higher w/c and to vary the dosage of the hydrophobic chemical admixtures. The higher w/c accommodated the reduction of another variable, the removal of superplasticizer from the recipe. Differences in the thicknesses of the concrete were also investigated as the time to reach a stable weight at 40°C was long (ca six months). Below in FIGURE 4.4, one can find the effect of incremental increases of an unprocessed TAG (O.O.) on water absorption.

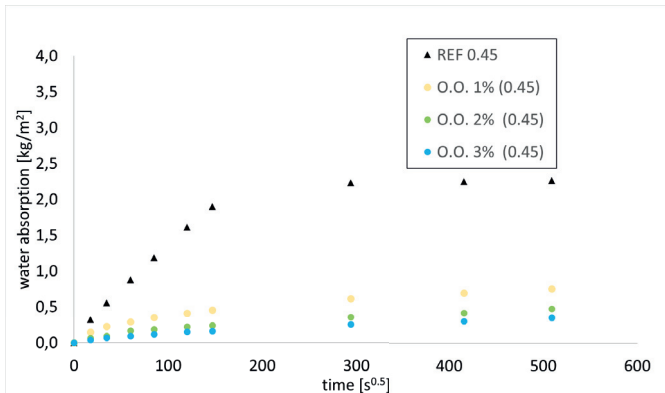


FIGURE 4.4. Water absorption of concrete discs (thickness 20 mm) O.O. 1-3% (0.45) without air entrainer (AE) or superplasticizer (SP).

Here, one can observe a drop in water absorption rates with the increase in the hydrophobic chemical. The decrease is not linear. These results are representative of all the other hydrophobic chemicals and can be seen in APPENDIX 3 and all coefficients, W_{w24} , can be seen in TABLES 4.6 (20 mm thick specimens) and 4.7 (80 mm thick specimens).

TABLE 4.6. Results of water absorption coefficients from concrete $w/c = 0.45$ (20 mm thick discs)

Concrete recipe	W_{w24} [kg/(m ² h ^{1/2})]	Reduction in [%] compared to REF (0.45)
REF (0.45)	0.776	
O.O. 1% (0.45)	0.126	-83
O.O. 2% (0.45)	0.072	-90
O.O. 3% (0.45)	0.052	-93
R.S.O. 1% (0.45)	0.187	-75
R.S.O. 2% (0.45)	0.088	-88
R.S.O. 3% (0.45)	0.059	-92
C.H.A 2 1% (0.45)	0.110	-85
C.H.A 2 2% (0.45)	0.060	-92
C.H.A 2 3% (0.45)	0.050	-93

TABLE 4.7 Results of water absorption coefficients from concrete $w/c = 0.45$ (80 mm thick cylinder)

Concrete recipe	W_{w24} [kg/(m ² hr ^{1/2})]	Reduction in [%] compared to REF (0.45) BIG
REF (0.45) BIG	0.906	
O.O. 1% (0.45) BIG	0.171	-81
O.O. 2% (0.45) BIG	0.106	-88
O.O. 3% (0.45) BIG	0.075	-91
R.S.O. 1% (0.45) BIG	0.244	-73
R.S.O. 2% (0.45) BIG	0.128	-85
R.S.O. 3% (0.45) BIG	0.105	-88
C.H.A 2 1% (0.45) BIG	0.131	-85
C.H.A 2 2% (0.45) BIG	0.077	-91
C.H.A 2 3% (0.45) BIG	0.068	-92

4.1.2.3. Water absorption concrete 0.50

In a further expansion to the project, the concrete recipe was changed. The w/c was increased to 0.50, see TABLE 4.8, and the commercial product (C.H.A 2) was removed

from the matrix and replaced with >97% purity alkyl alkoxysilane products. Some variances in the type of alkyl alkoxysilane were also tested.

TABLE 4.8 Results of water absorption coefficients from concrete w/c = 0.50 (20 mm thick discs)

Concrete recipe	W_{w24} [kg/(m ² hr ^{1/2})]	Reduction in [%] compared to REF (0.50)
REF (0.50)	0.934	
O.O. 1% (0.50)	0.173	-81
O.O. 2% (0.50)	0.073	-92
O.O. 3% (0.50)	0.065	-93
R.S.O. 1% (0.50)	0.186	-80
R.S.O. 2% (0.50)	0.118	-87
R.S.O. 3% (0.50)	0.083	-91
n octyl 1% (0.50)	0.103	-88
n octyl 2% (0.50)	0.075	-91
n octyl 3% (0.50)	0.057	-93
IBES 1% (0.50)	0.074	-92
NOMS 1% (0.50)	0.069	-92

n-octyl = n-octyltriethoxysilane

IBES = Iso-butyltriethoxysilane

NOMS = n-octyltrimethoxysilane

The increase in water cement ratio increased the water absorption coefficient by ca 20% (based on similar thickness). The increase in hydrophobic admixture decreased the water absorption rate with all hydrophobic admixtures. At equal “silane” dosage rates, n-octyltrimethoxysilane (NOMS 1%) reduced its rate of water absorption the most of the three “silanes” in the test matrix.

4.2. Compressive strength

Compressive strengths of the mortars (w/c = 0.50) are presented in [77]. Observation of the data would conclude that all long-chained hydrocarbon additives reduced the compressive strengths. The addition of TAGs at 3% reduced the compressive strengths between 15 and 37%, the addition of commercial chemicals reduced the strengths by 37 to 70%. Ultrafine fillers increased the compressive strength.

A graph depicting the compressive strength from the initial concrete mixes for Nordic civil infrastructure (w/c = 0.40) is presented below in FIGURE 4.6. Thereafter, a general trend for all the concretes is presented showing the effect of w/c and % hydrophobic additives on the compressive strengths. For all the data please refer to APPENDIX 4.

4.2.1. Compressive strengths after 28 days - 3 years; concrete w/c = 0.40

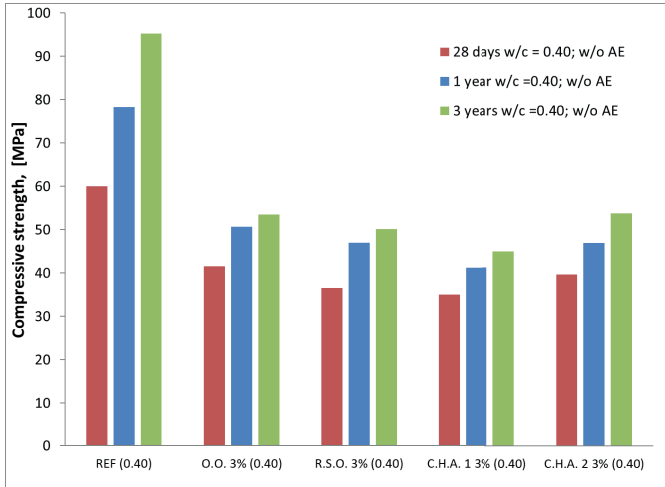


FIGURE 4.6. Compressive strength development of concretes, w/c = 0.40 without air entrainer. Hydrophobic admixture fixed at 3% (cement weight).

The results show a strong contrast between the compressive strength of treated concretes, i.e. with added hydrophobic chemicals, and the reference (REF). All concretes gain strength with time but the addition of these chemicals hinders the development.

4.2.2. General strength changes of all concretes with variable % hydrophobic additives at 28 days

A graph showing a general compressive strength trend is presented below in FIGURE 4.7.

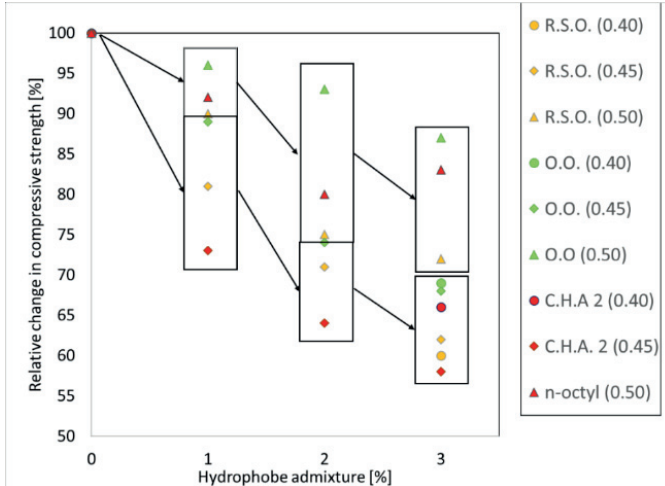


FIGURE 4.7. General trend of strength development after 28 days; all concretes; variable amount of hydrophobic additives. IBES and NOMS concrete not include. Triangle = 0.50 concretes; diamond = 0.45 concretes; circle = w/c = 0.40.

FIGURE 4.7 shows a downward compressive strength trend with increasing % addition of hydrophobic additives. From the available data, the higher the w/c the lower the relative compressive strength loss. No data for w/c = 0.40 at 1% and 2% are available, see TABLE 4.9. for summary.

The cold pressed unprocessed TAG (olive oil extra virgin) had the least impact on the compressive strengths even as the dose increases as shown by its higher positioning within the schematic rectangular boxes. The highly processed TAG (R.S.O.) lowers the relative compressive strength, which can be especially seen in the 0.50 series. Due to the change of “silane” product one cannot directly compare the 0.45 and 0.50 series.

TABLE 4.9. Compressive strength results from concrete $w/c = 0.45$; after 28 days-3 years

w/c = 0.45	28 days [MPa]	comp. to REF (0.45) [%]	1 year [MPa]	comp. to REF (0.45) [%]	3 years [MPa]	comp. to REF (0.45) [%]
REF (0.45)	59.0		79.9		79.2	
R.S.O. 1% (0.45)	48.0	-19	56.8	-29	62.2	-21
R.S.O. 2% (0.45)	41.7	-29	53.9	-33	58.5	-26
R.S.O. 3% (0.45)	36.4	-38	47.4	-41	54.5	-31
O.O. 1% (0.45)	49.5	-16	61.4	-23	67.0	-15
O.O. 2% (0.45)	43.4	-26	54.3	-32	58.8	-26
O.O. 3% (0.45)	40.1	-32	50.5	-37	56.3	-29
C.H.A. 2 1% (0.45)	42.8	-27	53.2	-33	58.7	-26
C.H.A. 2 2% (0.45)	36.4	-38	50.3	-37	53.2	-33
C.H.A. 2 3% (0.45)	34.5	-42	47.4	-41	47.4	-40

TABLE 4.10. Compressive strength results from concrete $w/c = 0.50$; after 28 days – 3 years

w/c = 0.50	28 days [MPa]	comp. to REF (0.45) [%]	1 year [MPa]	comp. to REF (0.45) [%]	3 years [MPa]	comp. to REF (0.45) [%]
REF (0.50)	41.0		65.8		71.5	
R.S.O. 1% (0.50)	37.0	-10	53.3	-19	60.3	-16
R.S.O. 2% (0.50)	30.8	-25	46.0	-30	49.3	-31
R.S.O. 3% (0.50)	29.7	-28	45.4	-31	49.0	-31
O.O. 1% (0.50)	39.5	-4	56.1	-15	60.6	-15
O.O. 2% (0.50)	38.0	-7	49.6	-25	55.7	-22
O.O. 3% (0.50)	35.6	-13	46.9	-29	48.8	-32
n-octyl 1% (0.50)	37.7	-8	53.8	-18	56.0	-22
n-octyl 2% (0.50)	32.6	-20	49.6	-25	53.2	-26
n-octyl 3% (0.50)	34.1	-17	47.8	-27	52.1	-27
n-OMS 1% (0.50)	25.5	-38	34.8	-47	41.6	-42
i-BES 1% (0.50)	39.8	-3	58.7	-11	61.2	-14

4.3. Freeze thaw resistance of concrete

Freeze thaw resistance testing is an artificial and accelerated test to demonstrate cement paste's ability to redistribute forces which are created when solutions of water are cooled (frozen) and thawed within a 24-hour period over multiple days.

For the first set of results please refer to [78]. The results below in FIGURES 4.8 and 4.9 are a repeat of the testing of specimens in the same subset but are of course older.

A contrast between the first and second round of testing is evident. The first and second round of testing show that the alkyl alkoxy silane admixtures (C.H.A. 1 & 2) have a negative impact on freeze thaw resistance regardless of being placed in deionized water or 3% NaCl solution.

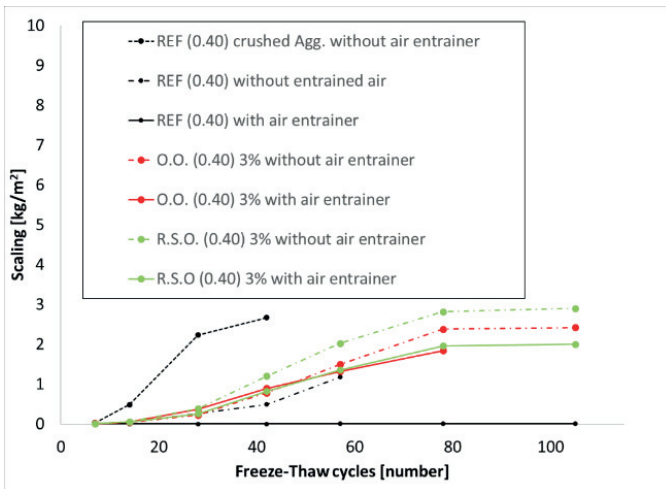


FIGURE 4.8. Freeze thaw results of concrete ($w/c = 0.40$) with addition R.S.O and O.O. (TAGs), with and without air entrainer. Included are also results from reference mixes with and without air entrainer. Tested in 3% NaCl solution.

After 56 cycles, all concretes except “REF (0.40) with air entrainer” are classified as “not valid” / “icke godkánt” as the scaling is $> 1.0 \text{ kg/m}^2$. The addition of air entrainer in R.S.O. (0.40) and O.O. (0.40) reduces the scaling in both cases (solid green and red lines) but is insufficient to reduce the scaling to the levels measured in “REF (0.40) with air entrainer”, see the solid black line on the x-axis.

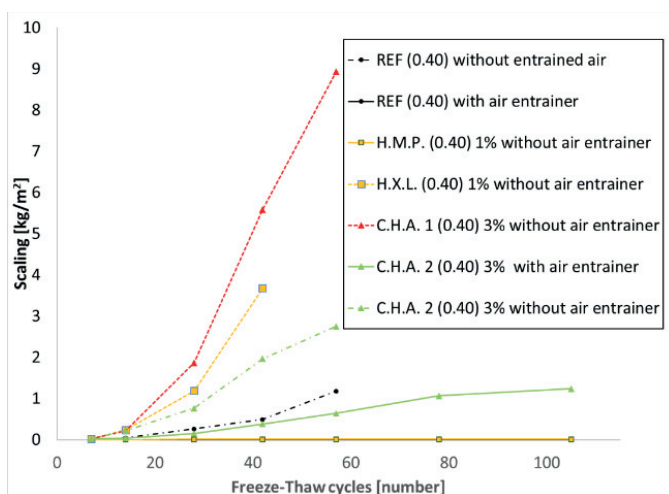


FIGURE 4.9. Freeze thaw results from concrete $w/c = 0.40$ with addition of commercial products, with and without air entrainer. Tested in 3% NaCl solution.

Thin sections of the concrete from the second round of freeze thaw can be seen in APPENDIX 1.

Cylindrical samples were extracted from the freeze thaw specimens from [78]. The compressive strength results can be found in APPENDIX 4.

4.4. Unidirectional chloride diffusion

Sawn concrete surfaces exposed to a 0.55 M NaCl solution with different % of hydrophobic admixtures were analyzed for the presence of chloride ions at millimeter incremental steps from the exposed surface. The concretes varied in w/c (0.45 and 0.50) and addition of hydrophobic admixtures (1-3%). The samples were nearly always in a saturated environment prior to exposure to the NaCl solution and the total exposure to which was 91 days.

At $w/c = 0.45$ and in the cement paste in the case of the triacylglycerols (TAGs), the higher the percentage admixture the lower the amount of chloride ions that were transported into the cement paste. In concretes with 1% admixture, (TAG or “silane”), no significant difference in amount of chloride ions entering the cement paste matrix compared to the reference could be graphically established. At 3% inclusion, the processed (refined, bleached and deodorized) oil (R.S.O) performed the best based on the graphical and mathematical results, followed by the unprocessed TAG (O.O.). The presence of “silane” in the cement paste increased the accumulated chloride ion content, see FIGURES 4.10 and 4.11 for generalizations observed from the results.

The slight increase in w/c to 0.50 provided for a higher mass transfer of chloride ions into the cement paste. Even at 3% inclusion of both TAGs, similar results to the reference to chloride ion diffusion could be measured. In the case of the 3% “silane” concrete specimen, even more chlorides were transported into the cement paste and further in from the exposed surface.

Based on the mathematical calculations for D_{adj} , from which one obtains a diffusion coefficient, the processed TAG (R.S.O.) performed better in the concrete with the lower w/c (0.45) than in the 0.50 concrete. This resulted in a 66 % reduction in the diffusion coefficient, followed by the unprocessed TAG (O.O.) with a 51% reduction. The diffusion coefficient in the concrete with C.H.A. 2 (“silane”) increased diffusion by 11%.

A similar pattern of chloride diffusion coefficient was seen in the higher w/c concrete (0.50) whereby O.O. resulted in a 60% reduction, R.S.O. (-54%) and NOTES/ n-octyl (-14%) relative to the reference concrete.

General trends of the different hydrophobic chemicals on the mass transfer of chlorides ions into cement paste are presented in the two following figures.

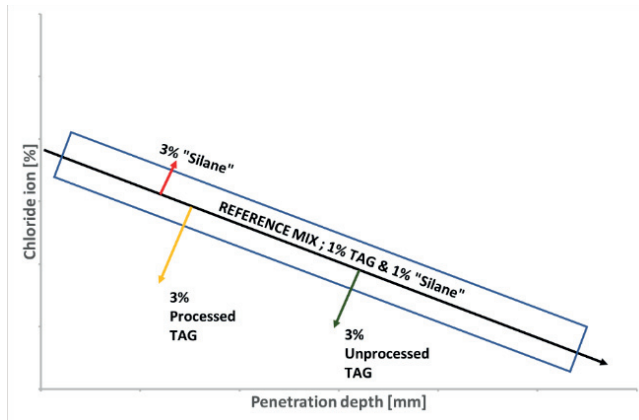


FIGURE 4.10. General observation in concrete chloride diffusion with w/c = 0.45.

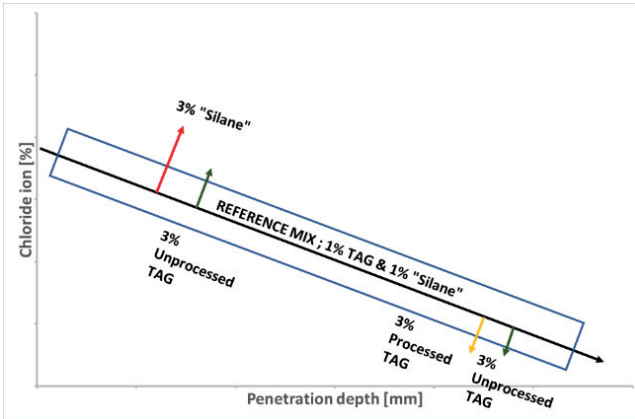


FIGURE 4.11. General observation in concrete chloride diffusion with $w/c = 0.50$.

4.5. Capillary absorption of Cl⁻; accelerated seasonal test

Eight artificial “years” were simulated as described in the METHODS Section. Four concrete specimens were exposed to a 3 % NaCl solution during the “winter” season. The concrete surfaces were never washed. The results from the chloride ion analysis at millimeter incremental depths of the four concrete specimens at cool temperatures are presented below in FIGURE 4.12.

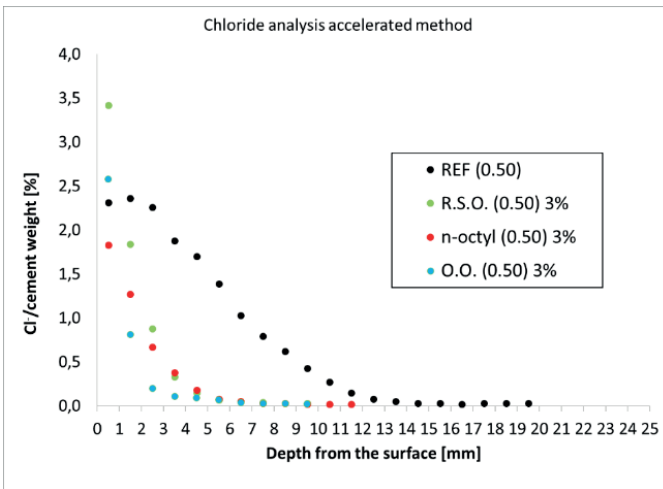


FIGURE 4.12. Measured chloride contents at different depths of concretes subjected to eight artificial seasons.

The typical chloride profile of a “normal” concrete exposed to chlorides in a fluctuating environment is obtained in the REF (0.50) data points. At approximately 14 mm, there are comparatively few chloride ions left in the cement paste. The addition of

hydrophobic chemicals (R.S.O, O.O. and n-octyl triethoxysilane) reduced the amount of mass transfer of chloride ions and it this was shown by the reduction of and depth at which chloride ions were detected, i.e. these changed the capillary action of the cement paste. At approximately 6-7 mm there are no differences between the three hydrophobic concrete specimens.

4.6. Isothermal calorimetry

4.6.1. w/c = 0.45 & 20 °C

Isothermal calorimetry is a useful tool to determine changes to “normal” cement mineral hydration (if any) in the initial 24-48 hours. A typical example of the hydration sequence can be seen in series “REF (0.45) 20 °C” in FIGURE 4.13. It represents the heat liberated from a cement paste during the initial hours whilst in the fresh state. A summary of the first and second heat flow peaks are presented in TABLE 4.11.

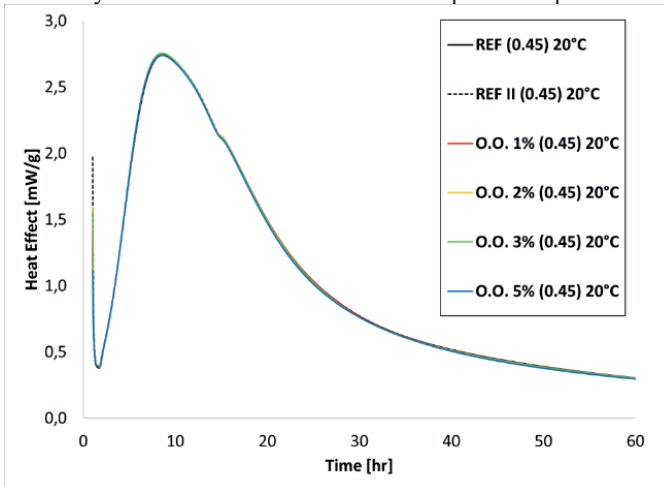


FIGURE 4.13. Results from iso thermal calorimetry experiment of CEM I 42,5 N LA/SR3/MH REF (0.45) 20 °C and unprocessed TAG (O.O.) at concentrations 1-5%.

The increase addition of unprocessed TAG (O.O.) to the cement paste did not significantly change the liberated heat rate at which the clinker minerals were hydrating. A slight increase of 0.5% can mathematically be detected on the first peak (at ca 10 hr). This was not the case with the processed TAG (R.S.O.) where an increase in the 1st and 2nd heat release phase could be detected. The alkyl alkoxy silane (n-octyl) cement pastes showed similar results as O.O., i.e. no change to the reference. These results are presented in APPENDIX 5.

An additional graph is presented below to show the effect glycerol has on cement mineral hydration. Glycerol and glycerol-like compounds such as diacylglyceride (DAG) or monoacylglyceride (MAG), are byproducts from the saponification of TAG. This chemical process happens in stages TAG->DAG->MAG. Should the TAG change

(saponify) then a change in the hydration process should be apparent. Below, in FIGURE 4.14, the molar equivalent of 1, 2 and 3 % TAG breakdown (complete) on the hydration of CEM I is presented.

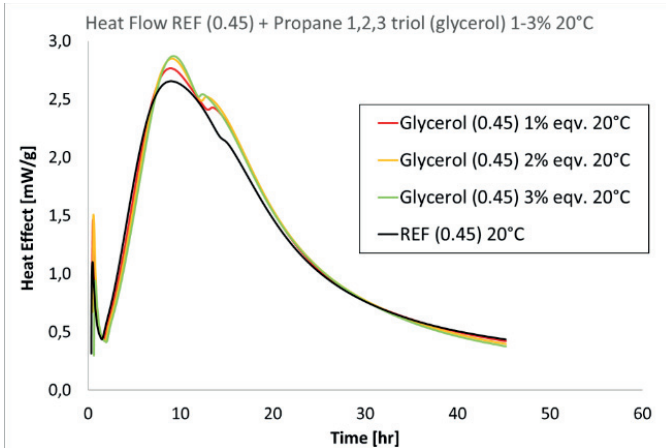


FIGURE 4.14. Results from iso thermal calorimetry experiment with the inclusion of propane 1,2,3 triol (glycerol) at 20 °C. The % is stoichiometric equivalent of the breakdown of 1-3 % TAG.

In FIGURE 4.14 one sees the effect glycerol has on the hydration energy released. The first and second peaks are affected. The effect is not linear, i.e. the rate change from 0-1% is higher than from 2-3%. The chemical process appears to be limited by an unknown factor.

4.6.2. w/c = 0.45 & 50 °C

The temperature of the iso thermal calorimeter was increased to a higher temperature one would expect in a hydrating concrete (upper end), increasing the temperature should also increase the rate or likelihood of saponification compared to 20 °C, the mixing technique remains the same. The time scale of testing is not important in this case as the base time for the equipment varies from measurement to measurement. Below, in FIGURE 4.15, the results from the unprocessed TAG (O.O.) testing at 50°C are presented. In FIGURE 4.16. the effect of propane 1,2,3 triol (glycerol) on the cement hydration is presented.

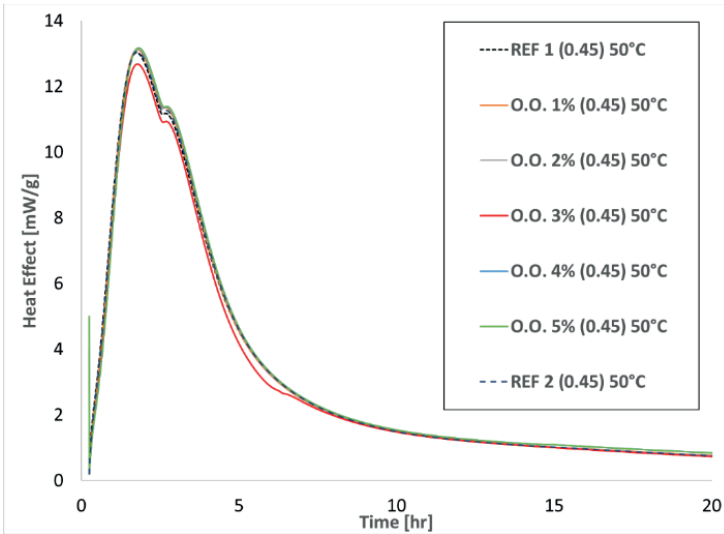


FIGURE 4.15. Results from iso thermal calorimetry experiments at 50 °C with the inclusion of unprocessed TAG (O.O.) Time 0-20 hrs.

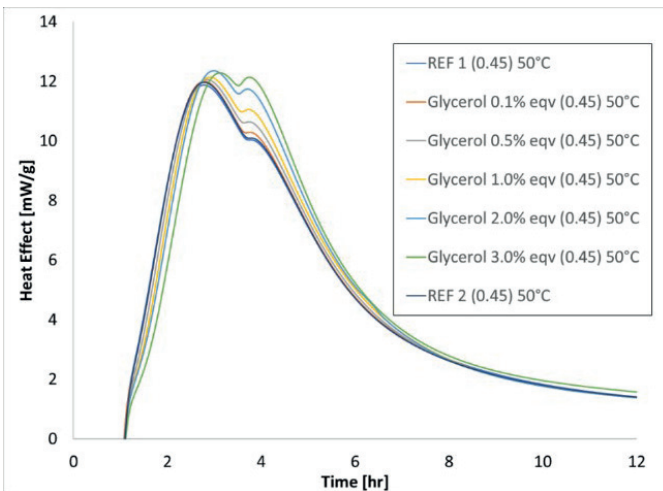


FIGURE 4.16. Results from iso thermal calorimetry experiment at 50 °C with the inclusion of propane 1,2,3 triol (glycerol). The scope of results was increased to cover 0.1 %- 3.0%.

The scales of both figures' x and y-axes have been changed from FIGURE 4.14 to reflect the higher amount of energy liberated over a shorter amount of time.

Results from O.O. 3% (0.45) in FIGURE 4.15 have been included despite a “drop” in heat liberated. The ampoule was exposed to a slight bump on the way to the calorimeter and approx. 0.3 g attached to the side walls, showing how sensitive the experiments are to slight deviations or material accumulation on the side walls.

Using the summaries from TABLE 4.11, the inclusion of unprocessed TAG (O.O.) caused a slight increase (+0.9%) in the liberated heat for the first peak and (+0.60 %) in the second peak. The increase in heat flow into the cement paste system did not significantly increase the rate of saponification or any other change in the TAG chemistry.

It is very interesting to note the rise in heat flows, both 1st and 2nd peak in the cement paste with the processed TAG, “R.S.O. X% (0.45) 50°C”, see TABLE 4.11. These are significantly higher than those obtained from the unprocessed TAG series (O.O.). The increase in heat flow is also progressive i.e., the more processed R.S.O. that was added, the higher the maximum heat flow registered.

In the “silane” (n-octyl) series no significant change in heat flow release was shown compared to the reference. The first peak shows a more responsive change with increasing “silane” content.

The propane 1,2,3 triol (glycerol) experiments, see FIGURE 4.16, show that the higher temperature has a significant effect on the cement hydration compared to at 20 °C. The increased heat energy from the surrounding environment accelerated the second peak significantly. One even notices a slight retardation effect on the first peak. Here, the increased amounts of glycerol increased the second peak in a more linear way compared when the experiment was conducted at 20 °C. The change of heat flow is more significantly placed on the second peak, where increasing the dosage increased the change in a more linear fashion. At 2% eqv., the first peak increased ca 4% and 17% for the second peak. As with the experiments at 20 °C, there seems to be a limiting factor once one adds the equivalent molar mass of glycerol of a complete chemical breakdown of 3% TAG.

Graphical results from the processed TAG (R.S.O.) and n-octyl (“silane”) are presented in APPENDIX 5.

TABLE 4.11 Results 1st and 2nd Peak from iso thermal calorimetry

	Experiment	1 st Peak [mW/g]	Change compared to REF [%]	2 nd Peak [mW/g]	Change compared to REF [%]
Glycerol 50 °C					
	REF 1(0.45)	11.87		10.02	
	Glycerol 0.1% eqv (0.45)	11.99	1.01	10.28	2.59
	Glycerol 0.5% eqv (0.45)	12.05	1.52	10.63	6.09
	Glycerol 1.0% eqv (0.45)	12.13	2.19	11.05	10.28
	Glycerol 2.0% eqv (0.45)	12.35	4.04	11.73	17.07
	Glycerol 3.0% eqv (0.45)	12.28	3.45	12.13	21.06
	REF 2(0.45)	11.95		10.09	
O.O. 50°C					
	REF 1 (0.45)	13.03		11.26	
	O.O. 1% (0.45)	13.20	1.31	11.41	1.33
	O.O. 2% (0.45)	13.13	0.75	11.35	0.80
	O.O.3% (0.45)	13.10	0.55	11.29	0.28
	O.O. 4% (0.45)	13.16	1.00	11.37	0.98
	O.O. 5% (0.45)	13.16	0.98	11.32	0.53
	REF 2 (0.45)	13.07		11.27	
n-octyl 50 °C					
	REF 1 (0.45)	13.65	0.00	11.98	0.00
	n-octyl 1% (0.45)	13.63	-0.15	12.03	0.42
	n-octyl 2% (0.45)	13.64	-0.07	12.01	0.25
	n-octyl 3% (0.45)	13.71	0.44	12.05	0.58
	n-octyl 4% (0.45)	13.73	0.59	12.09	0.92
	n-octyl 5% (0.45)	13.76	0.81	12.08	0.83
	REF 2 (0.45)	13.65		12.03	
	Experiment	1 st Peak [mW/g]	Change compared to REF [%]	2 nd Peak [mW/g]	Change compared to REF [%]
R.S.O 50 °C					
	REF (0.45)	13.82		12.20	
	R.S.O. 1% (0.45)	14.03	1.52	12.51	2.54
	R.S.O. 2% (0.45)	14.09	1.95	12.62	3.44
	R.S.O. 3% (0.45)	14.23	2.97	12.75	4.51
	R.S.O. 4% (0.45)	14.19	2.68	12.75	4.51
	R.S.O. 5% (0.45)	14.25	3.11	12.80	4.92
	REF 2 (0.45)	13.85		12.25	

Temp: 20 °C		1 st Peak [mW/g]	Change compared to REF [%]	2 nd Peak [mW/g]	Change compared to REF [%]
O.O.					
	REF 1(0.45)	2.74	0.00	2.13	0.00
	O.O. 1% (0.45)	2.75	0.34	2.14	0.38
	O.O. 2% (0.45)	2.75	0.47	2.14	0.36
	O.O. 3% (0.45)	2.76	0.50	2.14	0.35
	O.O. 5% (0.45)	2.74	-0.06	2.13	0.09
	O.O. 10% (0.45)	2.69	-1.87	2.13	-0.21
	REF 2 (0.45)	2.75	0.23	2.10	-1.43
R.S.O					
	REF 1 (0.45)	2.75		2.26	
	R.S.O. 1% (0.45)	2.78	1.09	2.28	0.88
	R.S.O. 2% (0.45)	2.80	1.82	2.31	2.21
	R.S.O. 3% (0.45)	2.81	2.18	2.32	2.65
	R.S.O. 4% (0.45)	2.85	3.64	2.35	3.98
	R.S.O. 5% (0.45)	2.82	2.55	2.33	3.10
	REF 2(0.45)	2.75		2.26	
Glycerol					
	REF (0.45)	2.66	0.0	2.16	0.0
	Glycerol 1% eqv. (0.45)	2.76	4.0	2.42	12.0
	Glycerol 2% eqv. (0.45)	2.85	7.4	2.52	16.7
	Glycerol 3% eqv. (0.45)	2.88	8.3	2.52	16.7
n-octyl					
	REF (0.45)	2.69	0.0	2.08	0.0
	n-octyl 1% (0.45)	2.60	-3.4	2.03	-2.4
	n-octyl 2% (0.45)	2.67	-0.7	2.14	2.9
	n-octyl 5% (0.45)	2.70	0.4	2.10	1.0

4.7. Field station

The field station has been installed since 18th January 2018 and has two rounds of samples placed in each position. There are no chemical or physical results from the field station except observations in terms of the state of the exposed surface. The field station is photographed and inspected annually and has to date not shown any signs of surface deterioration. Digital photos of the field station can be seen in APPENDIX 6.

5. DISCUSSION

The main aim of this work was to evaluate and measure the effectiveness of different potential hydrophobic admixtures in fresh concrete in order to increase durability of the hardened product. These should provide a homogenous hydrophobic bulk effect in the hardened product (concrete). This addition in the fresh concrete would then negate the need to apply a protective coating in concrete structures subjected to harsh environments, e.g. edge beams. The depth of penetration and the durability of the externally treated concrete surfaces would subsequently not be an issue. Some of the bulk hydrophobic concretes investigated had sufficient reduction in water absorption and could potentially be applied in a Nordic infrastructural environment. Below, the different aspects of the testing are discussed.

5.1. Compressive strength

The compressive strength results show a repetitive pattern: The addition of triacylglycerides (TAG) or alkyl alkoxysilane based hydrophobic agents reduces the relative compressive strength of the concrete. This was also true for results from [77], where even the type and combination of the mainly C_{18:n} fatty acid (saturated, mono- or di unsaturated) on the esterified propane-1,2,3-triol backbone effected the compressive strength. The least negative outcome was observed in the unprocessed TAG (extra virgin olive oil). A general feature of this being a high oleic acid content (cis-9-octadecenic acid) on its glycerol backbone compared to the other TAGs. As the product is only lightly processed, additional chemicals are still present, such as free fatty acids (e.g. oleic acid) and other minor components.

The range of additions in this study was limited to four intervals 0, 1, 2 & 3% based on cement weight. Each additional increase resulted in a lower average strength. Three w/c ranges were covered but more extensively in the 0.45 – 0.50 range. The relative strength drop decreased with increasing w/c, i.e., at equal dosages of hydrophobic admixture, the concrete with the lower w/c will have a relatively lower compressive strength.

In [49] only minor drops in compressive strength was shown (10 and 19 %) with w/c = 0.40 and inclusion of 1 and 2% of a processed TAG respectively. In [48] a larger drop (30%) in compressive strengths were observed in mortar samples after three years, but the dosages covered only 0.5, 1.0 & 1.5%. Others have investigated hardened cement pastes [54] and concluded the same. A multitude of theories e.g., mineralogical changes due to the production of calcium glycerate, C-S-H structural changes or degree of hydration etc., are but some of the explanations given to these changes in mechanical strength.

Heat flows from the iso thermal calorimeter of the processed TAG (R.S.O.) showed a significant increase compared to the unprocessed TAG. The formation of a weaker and more water-soluble mineral such as calcium glycerate as demonstrated in [75] may be the cause of one of the observations from this work i.e., the compressive strength of all

concretes tested were weaker with the inclusion of R.S.O than with O.O. This though only explains the effect of TAGs on the cement paste structure and not the alkyl alkoxysilanes which have a similarly negative effect on strengths.

Specimens for compressive strengths and freeze thaw testing were cast in plastic moulds compared to the thick metal cylinder moulds for the chloride diffusion testing. The heat conduction of plastic is significantly lower than that of metal which would increase the core temperature of the young concrete. This factor has not been taken into consideration in the results, a lower cement paste temperature should reduce the effects of saponification or the formation of weaker clinker minerals in the processed TAG. More experimental work is required to verify this.

In general, the “silane” based admixtures have a similar negative effect on the compressive strength development in concrete. The hydrolysis of alkyl alkoxysilane to a related siloxane in a high pH environment is fast and requires water. The hydration of cement clinker minerals requires water as well. The two can compete, which was apparent when the alko group in the chemical was substituted from n-octyltriethoxysilane to an n-octyltrimethoxysilane. Insufficient “free” water was available for compaction and the compressive strength was reduced considerably. The addition of heat did not affect heat flow of cement pastes with “silane” indicating no change to the cement clinker hydration rate. XRD analysis would be further required to confirm this statement.

5.2. Water absorption from oven dry state (40 °C)

The initial mortar testing was to screen out hydrophobic admixtures and their efficiencies. The “silane” based admixtures were more effective than the other commercial products.

Within the TAGs, which all performed well, the highest water absorption reductions were observed in the mortars with extra virgin olive oil, sesame oil and rape seed oil. Limited sesame oil production volumes and higher cost were disadvantageous compared to rape seed oil and consequently they were eliminated from the continuation of the study.

All concretes with the screened admixtures performed well from an oven dried state with at least a 75% reduction in the water absorption coefficient, W_{w24} . This was the case with series R.S.O 1% (0.45) compared to the reference. The reduction range for all specimens was 75-93%.

In general, the differences in water absorption between the hydrophobic chemicals are most noticeable at the lower admixture rates (1%). At higher rates e.g., 3%, the difference between the W_{w24} results differed only $\pm 2\%$. The unprocessed TAG (extra virgin oil) performed better than the processed TAG (rape seed oil).

The comparison between the thin (20 mm) concrete specimens and the large cylinders (80 mm) showed that in all cases, the water absorption coefficient, W_{w24} , was always higher in the larger specimen but the preparation time is considerably longer, six months (80 mm) compared to ca 1.5 months (20 mm).

5.3. Freeze thaw resistance

The repetition of the freeze thaw (F-T) testing in the NaCl solution presented two significant outcomes. According to [78] the use of TAG in the cement paste presented no challenges to the concrete's resistance to scaling during the testing. Repeating the testing though, as presented in the RESULTS Section showed the opposite. Only one concrete with the hydrophobic admixture. H.M.P (0.40), cleared the $<1.0 \text{ kg/m}^2$ scaling criterion. Its chemistry was suitable to create sufficient and correctly sized air pores, see APPENDIX 1 (thin section).

The TAG based cement pastes, where the air entrainer was stable and sufficient, see APPENDIX 1 (thin section), was insufficient to prevent large scaling on the exposed concrete's surface. The inclusion of air pores did however prevent parallel crack formations which could be seen in the TAG cement pastes without air entrainment. Testing F-T in deionized water was not as harsh and resulted in less scaling, this test was not repeated.

A general trend in the TAG concretes with air entrainer, was that it performed better than without. All values were under 0.25 kg/m^2 after 91 days, which is considered as "good" scale resistance.

The inclusion of "silane" in the fresh concrete has an extremely negative effect on F-T resistance, which was seen in [78] and in the repeat testing. This was even the case in testing the exposed concrete surface to deionized water, which usually is a "milder" form of freeze thaw resistance testing. This resulted in a scale resistance between $0.22\text{-}0.47 \text{ kg/m}^2$ after 91 cycles.

More research is required to understand the dynamics during F-T cycling on cement pastes with bulk hydrophobic agents. The above observations were limited to a Nordic bridge concrete recipe ($w/c = 0.40$) with the inclusion of 3% hydrophobic admixture. It is possible that the percentage of admixture was too high for this particular w/c , causing mass transfer issues in the cement paste pore system. Lower inclusion rates should be investigated.

5.4. Unidirectional chloride ion diffusion

The use of different TAGs, which in this study was rape seed oil (R.S.O.) and extra virgin olive oil (O.O.), produced different resistances of the concrete to hinder mass transfer of chloride ions from the surface and inwards. This effect though could only be measured if high admixture amounts (3% of cement weight) were included in the

cement paste matrix. At 1%, no substantial difference could be seen in the chloride analysis between the treated and reference concrete.

Inclusion of an alkyl-alkoxysilane was less effective in preventing Cl⁻ diffusion in a near saturated concrete. It could even be seen as a negative factor if sufficiently high amounts were added.

5.5. Capillary absorption of Cl⁻, accelerated method

All three concretes with bulk hydrophobic admixtures (3%) performed better than the reference, which can be seen very clearly in the chloride ion vs depth analysis, see FIGURE 3.2 The absence of any type of washing of the specimens and the horizontal placing during the “winter” season provided a harsh environment. It would be interesting to test concretes at lower admixture levels to find an optimum inclusion rate with regard to resistance to capillary mass transfer mechanisms.

The method by which the water solution (and the Cl⁻) are prevented from entering the pore system is due to the hydrocarbon chains repelling the dissolution of water molecules. From previous results, see Water absorption from oven dried state, the internal relative humidity (RH) was particularly low and good results were obtained. In these experiments the surface RH is higher, approx. 85%, but the capillary repelling action is sufficient to significantly reduce the mass flow of external solutions (water based) inwards.

This external mass flow reduction though is only effective when the pores are not saturated, as one can see in the results from Section 3.4. Here, capillary wall based hydrophobic admixtures were not as effective when the capillary pores were saturated allowing for the ions to be transported outside of the “reach” of polymer siloxane in the pores’ internal volume.

5.6. Iso thermal calorimetry

Cement pastes with different admixture levels and types were tested to see if their interactions changed the heat flow in the early stages of hydration. A mix with propane 1,2,3 triol (glycerol) was also used to demonstrate the effect any saponification of the TAG would have on the first and second heat flow peaks. The results from the added glycerol show an increase in heat flow at both temperatures, 20 °C and 50 °C. At 20°C, the increase is ca 8% and 16% on the first and second peak respectively. This changes at 50 °C where the increase is ca 4% & 22% on the first and second peak respectively.

TAG (unprocessed) olive oil: At 20 °C no significant rate change could be detected, the heat flow followed that of the reference cement (CEM I 42,5 N LA/SR3/MH). At 50 °C, the first and second peaks were slightly affected but only in the region of +0.50-0.98%.

TAG (processed) rape seed oil: At 20°C, a linear increase in first peak and second heat flow peaks are observable up to 4%. At 50 °C this trend persists and is significantly

higher than the reference at ca 3% (first peak) and ca 5% (second peak). This would indicate a higher degree of saponification and release of free fatty acids into the cement paste. It would be reasonable to deduce that this could lead to the formation of undesirable minerals and or the weakening of the microstructure. This could be an explanation as to the lower compressive strengths in the concretes with processed TAG than unprocessed TAG.

The n-octyl triethoxysilane had no particular effect on the heat flows of the hydrating cement paste at 20 °C nor 50 °C. The creation of ethanol and its subsequent evaporation (endothermic) though should have affected the heat flow in the calorimeter. This is not the case and any exothermic reactions taking place at the same time may mask this effect.

It was outside the scope of the study, but some input from [76] may explain some of the chemical interactions that occur using “silanes” in a cement paste (the study though was on a hardened synthetic cement paste).

6. CONCLUSIONS

To improve durability, bulk hydrophobic concretes were produced and tested for relevant aspects for Nordic conditions.

A common denominator for these hydrophobic additives is their long chain hydrocarbon group(s), which reduces the electro negativity (charge) across the molecule, preventing water from dissolving in them. This is the reason why these chemicals are effective in reducing the liquid flow of water in the pore system within a cement paste.

6.1. Water absorption

Experimental work has shown that the water absorption coefficient, W_{w24} , from oven dry (40 °C) concrete with 1% bulk hydrophobic chemicals can be reduced by 75% and as high as 93% with 3% addition compared to the reference concrete. The alkyl alkoxy silane based products are slightly better than the best performing TAG (O.O.).

Incremental increases of these chemicals, i.e. from 1%→2%→3%, reduces the water absorption rate further but this is not a linear relationship. The increase diminishes with increasing addition.

6.2. Compressive strength

The mechanical strength of the concrete is reduced with the inclusion of these hydrophobic chemicals. The higher the dosage the lower the strength. This relationship is not linear. The largest effect was noted between 0% and 1%. The decrease between 2% and 3% does not follow the steep decrease of the initial dosage (i.e. 1%). The effect of water to cement ratio (w/c) with similar dosages show that the higher the w/c, the lower the relative compressive strength drop.

All concretes gained strength with time within the scope of the study i.e. three years.

The TAGs used in the concrete recipes, whilst chemically similar (same chemical backbone and some of the hydrogen carbon groupings) do result in different physical properties in concrete. The unprocessed TAG (O.O.) always had higher compressive strength than the highly processed TAG (R.S.O.) with comparable concrete recipes.

Alkyl alkoxy silanes, like TAGs, have a negative impact on compressive strengths in concrete. The following sequence reflects the chemicals' impact from least to most negative on strengths Iso butyltriethoxysilane (i-BES) < n octyltriethoxysilane (n-octyl) < n-octylmethoxysilane (NOMS).

6.3. Freeze thaw resistance

The main issue arising within this work was the cement paste's freeze thaw (F-T) resistance in cases with the inclusion of hydrophobic chemicals. The addition of alkyl alkoxy silanes was extremely negative for concrete F-T resistance even when exposed to deionized water. TAGs and in particular the rape seed oil (R.S.O.) was promising according to [78]. Repetition of the specimens showed a less favorable conclusion. Further investigation is required to understand the mechanisms that prevent the air entrainers to work or the flow of water and or ions in the pore system when hydrophobic chemicals are present at low temperatures.

6.4. Chloride diffusion

Positive results were obtained when TAGs were included into the cement paste, a minimum amount is required, though, to obtain any benefits. Only slight benefits were noticed at 1% addition. The effects were more noticeable at 3%. R.S.O. functioned best based primarily on the visual results from the chloride ion depth profile. Similar dosages at different w/c do not have the same diffusion rate but have a similar percentage reduction compared to the reference. One must increase the dosage of hydrophobic additives to see any hindering effect if w/c is increased. This cannot be said of the alkyl alkoxy silanes, where higher or similar chloride ion profiles were measured as in the reference.

Mathematically, the unprocessed TAG (O.O.) had a higher resistance to chloride ion diffusion, $D_{adj\ 5mm}$ which was ca 50% lower than the reference.

6.5. Capillary absorption

Even though this test was limited (one set; w/c = 0.50 and 3% hydrophobic addition) compared to most other experimental results, the findings were relevant. The cement paste, even with its hydrophobic additions, did not prevent the ingress of chloride ions into the cement paste, even when the surface was exposed to RH 85%. They did though reduce the capillary mass transfer of chloride ions. The following are ranked (1st, 2nd and 3rd) in terms of their performance: unprocessed TAG (O.O.) -> n octylmethoxy silane (n-octyl) -> processed TAG (R.S.O.).

6.6. Iso thermal calorimetry

The inclusion of unprocessed TAGs or alkyl alkoxy silanes (n-octyltriethoxy silane) had no significant effect on the calorimetric reactions at 20°C, even over an extended range from 0 to 5%. The processed TAG (R.S.O.) did change the thermodynamics of the cement hydration which peaked at a 4% inclusion rate. Changes in the hydration phases (i.e. changes in the liberated heat rate) were detected when stoichiometric equivalent amounts of glycerol were added, even at 20°C. At 50°C, no significant change in

liberated heat was measured in unprocessed TAG (O.O.), this was not the case with the highly processed TAG (R.S.O.). The amount of heat liberated in the second phase increased and is not too dissimilar to that observed with glycerol. This could be a sign of the chemical breakdown of some of the triacylglycerides into free fatty acids and di- and monoglycerol.

6.7. Overall conclusion

One of the main degradation mechanisms of reinforced concrete is chloride induced corrosion of the rebars. This study showed that the interactions at the surface (capillary suction action) and further in at depths where rebar is placed (diffusion) can be altered to reduce the influx of chloride ions significantly with TAGs. This, though, requires an optimum admixture amount.

The use of alkyl alkoxysilanes as a bulk hydrophobic agent was negative, though, with regards the diffusion mechanism. It performed well when capillary suction action was tested.

Mechanical strength in concretes is mainly determined by w/c , which is normally a chosen value based on the concrete's surrounding environment, e.g., exposure to cyclical saline conditions. The required mechanical strength, though, could be lower than what the w/c , in time, accomplishes. In this respect the hydrophobic agents could be employed successfully despite the drop in mechanical strengths.

Despite the results from F-T testing, TAGs show potential to enhance the durability of concrete in respect to reducing chloride ion mass transfer.

7. REFERENCES

1. Rombén, L., *Alkaliballastreaktioner in Betonghandboken- Material* Ljungkrantz C., Möller G., and Petersons N., Editors. 1994, AB Svensk Byggtjänst: Stockholm pp 820-823.
2. Taylor H.F.W., *Cement Chemistry*. 1990, London: Academic Press Limited.
3. SIS, *SS-EN 197-1:2011 "Cement-Part 1: Composition, specifications and conformity criteria for common cements"*. 2011, SIS Förlag AB ; Swedish Standards Institute: Stockholm.
4. Hewlett, P.C., ed. *Lea's Chemistry of Cement and Concrete* 4ed. 1998, Arnold: London.
5. Ljungkrantz, C., Möller, G. and Petersons, N., eds. *Betonghandbok, Material* 2ed. 1994, AB Svensk Byggtjänst: Stockholm.
6. Scrivener K.L., *The development of microstructure during the hydration of Portland cement*. 1984, Imperial College London: <https://spiral.imperial.ac.uk/handle/10044/1/8567>.
7. Winslow D.N. and Diamond S., *A Mercury Porosimetry Study of the Evolution of Porosity in Portland Cement* 1969. 88.
8. Mehta P.K. and Monteiro P.J.M., *Microstructure of Concrete*, in *Concrete: Microstructure, Properties, and Materials*. 2014, McGraw-Hill Education: New York.
9. Glasser, F.P., *Role of Chemical Binding in Diffusion and mass transport*, in *Materials Science of Concrete Special Volume Ion and Mass Transport in Cement-Based Materials*, Hooton, R.D., Thomas M. D. A. and Marchand, J., Beaudoin J. J., Editors. 2001, Amer Ceramic Society, Ohio. pp. 129-154.
10. Winston Revie R. and Uhlig H.H., *Iron and Steel*, in *Corrosion and Corrosion Control*. 2008, John Wiley & Sons. pp. 115-145.
11. Camitz G., *Korrosionsskydd av stål i betongkonstruktioner Handbok*. 2011, Stockholm: Swerea KIMAB. 136.
12. Revie R.W. and Uhlig H.H., *Effect of pH*, in *Corrosion and Corrosion Control - An Introduction to Corrosion Science and Engineering (4th Edition)*. 2008, John Wiley & Sons: New Jersey. pp. 120-123.
13. Angst, U., Elsener, B., Larsen, C.K., and Vennesland, Ø., *Critical chloride content in reinforced concrete — A review*. *Cement and Concrete Research*, 2009. 39(12): pp. 1122-1138.
14. Page C.L. and Treadaway K.W.J., *Aspects of the electrochemistry of steel in concrete*. *Nature (London)*, 1982. 297(5862): pp. 109-115.
15. Creighton H.J.M., *Reinforced concrete versus salt, brine, and sea-water*. *Transactions of the Faraday Society*, 1919. 14: pp. 155-162.
16. RSA, *ENGINEERING NOTES; "The seasoning of concrete by calcium chloride"*. *Journal of the Royal Society of Arts*, 1916. 64(3334): p. 805.
17. López-Ortega A., Bayón R., and Arana J.L., *Evaluation of Protective Coatings for High-Corrosivity Category Atmospheres in Offshore Applications*. *Materials*, 2019. 12(8).
18. Luping T., Nilsson L.-O., and Basheer P.A.M., *Chloride transport in concrete*, in *Resistance of concrete to chloride ingress*. 2012, Spon Press: Oxon, UK.
19. Luping T., Nilsson L.-O., and Basheer P.A.M., *Modelling of chloride ingress in Resistance of concrete to chloride ingress; Testing and Modelling* 2012, Spon Press. pp. 75-119.
20. Nguyen H.T., Jacobsen S., and Melandsø F., *Capillary suction model as pipes of different sizes: flow conditions and comparison with experiments*. 2012. Trondheim: RILEM.
21. Betongförening, *Vägledning för livslängddimensionering av betongkonstruktioner* 2007, Betongföreningen.
22. Chatterji S. and Kawamura M., *Electrical double layer, ion transport and reactions in hardened cement paste*. *Cement and Concrete Research*, 1992. 22(5): pp. 774-782.
23. Friedmann H., Amiri O., and Ait-Mokhtar A., *Physical modeling of the electrical double layer effects on multispecies ions transport in cement-based materials*. *Cement and Concrete Research*, 2008. 38(12): pp. 1394-1400.
24. Pettersson K., *Olika faktors inverkan på kloriddiffusion i betongkonstruktioner*. 1994, Stockholm: Cement och Betong Institutet. 37.
25. Boverket, *Boverkets föreskrifter och allmänna råd om tillämpning av europeiska konstruktionsstandarder (eurokoder)*, C. Olsson, Editor. 2011. pp. 67-68.

26. Poursaeed A., *Corrosion of steel in concrete structures*, in *Corrosion of Steel in Concrete Structures*, A. Poursaeed, Editor. 2016, Woodhead Publishing: Oxford. pp. 19-33.
27. Ahmad S., *Reinforcement corrosion in concrete structures, its monitoring and service life prediction—a review*. Cement and Concrete Composites, 2003. **25**(4): pp. 459-471.
28. Gjörv O.E., *Steel corrosion in concrete structures exposed to Norwegian marine environment*. Concrete International 1994. **16**(4): pp. 35-39.
29. Hoar, T.P., *Report of the committee on corrosion and protection : A survey ... in the United Kingdom*. 1971, London: London..
30. Schmitt G., *Global Needs for Knowledge Dissemination, Research, and Development in Materials Deterioration and Corrosion Control*. 2009 [cited 2021 Available from: https://corrosion.org/Corrosion+Resources/Publications/_/whitepaper.pdf].
31. Koch, G.H., Brongers, M.P.H., Thompson, N.G., Virmani, Y.P., and Payer, J.H., *Corrosion Costs and Preventative Strategies in the United States*. 2001, Federal Highway Administration: Washington D.C ,USA. p. 12.
32. ASCE. *2021 Report card for America's infrastructure; Bridges*. 2021 [cited 2021 31 12 2021]; Available from: <https://infrastructurereportcard.org/wp-content/uploads/2020/12/Bridges-2021.pdf>.
33. Granger, F., ed. *On architecture* [Electronic resource] [2] Books VI-X. 1934, Harvard University Press: Cambridge, Mass.
34. Stymne S. and Stobart A.K., *8 - Triacylglycerol Biosynthesis*. 1987, Elsevier Inc. pp. 175-214.
35. Sickels L.B., *Organics vs synthetics : their use as additives in mortars*, in *Mortars, Cements and Grouts used in the Conservation of Historic Buildings*. 1981, ICCROM: Rome. pp. 25-52.
36. Jü. *Triglycerid-Strukturformel*. 2017 [cited 2021; Available from: <https://commons.wikimedia.org/w/index.php?curid=57095440>].
37. Fessenden R.J., *Organic chemistry*. 6th ed, ed. M.W. Logue and J.S. Fessenden. 1998, Pacific Grove, CA , USA
38. Blanco A. and Blanco G., *Chapter 5 - Lipids*, in *Medical Biochemistry*, A. Blanco and G. Blanco, Editors. 2017, Academic Press. pp. 99-119.
39. Perry, R.H. and Green, D.W., eds. 7th ed. *Perry's Chemical Engineers' Handbook* 1997, McGraw Hill.
40. Raygorodsky I., Kopylov V., and Kovyazin A., *2 Organosiloxanes (Silicones), Polyorganosiloxane Block Copolymers; synthesis, properties, and gas permeation membranes based on them*, in *Membrane Materials for Gas and Vapor Separation - Synthesis and Application of Silicon-Containing Polymers*, Y.F. Yampolskii, E., Editor. 2017, John Wiley & Sons.
41. Chandra G., *Organosilicon Materials*. Vol. 3 / 3H. 1997, Berlin, Heidelberg: Springer Berlin / Heidelberg.
42. Arkles B., *Tailoring Surfaces with Silanes*. Chemtech 1977. **7**: pp. 766-778.
43. Selander A., *Hydrophobic Impregnation of Concrete Structures-Effects on Concrete*, in *Structural Engineering*. Doctoral thesis 2010, Royal Insitute of Technology, KTH, Stockholm.
44. Leigh G.J., *Principles of chemical nomenclature : a guide to IUPAC recommendations*. 2011 edition.. ed. 2011, Cambridge: Cambridge : Royal Society of Chemistry.
45. Nora, A. and G. Koenen, *Metallic Soaps*, in *Ullmann's Encyclopedia of Industrial Chemistry*. 2010.
46. Justnes, H., *Low water permeability through hydrophobicity*, COIN Project report no. 1: SINTEF 2008
47. Justnes, H., Ostnor, T. A., and Barnils Vila, N., *Vegetable Oils as Water Repellents for Mortars*, in *1st International Conference of Asian Concrete Federation* 2004: Chiang Mai , Thailand. pp. 689-698.
48. Vikan H. and Justnes H., *Influence of Vegetable Oils on Durability and Pore Structure of Mortars*, in *7th CANMET/ACI International Conference on Durability of Concrete*. 2006, ACI Montreal, Canada. pp. 417-430.
49. Baghban, M.H., Hesselberg, E., Javadabadi, M.T., and Holvik, O.K., *Cementitious Composites with Low Water Permeability through Internal Hydrophobicity*. Key Engineering Materials, 2018. **779**: pp. 37-42.

50. Job, O.F., Achuenu, E., Maxwell, S.S., and Itodo, S.A., *Performance of Castor Oil as Admixture in Fresh Cementitious Matrix*. International Journal of Civil Engineering, 2017. 4(6): pp. 86-93.
51. Klieger, P. and Perenchio, W., *Freezing and thawing of concrete and use of silicones*. Highway Research Board, 1963(18): pp. 33-47.
52. Ma, Z., Wittmann, F.H., Xiao, J., and Zhao, T., *Influence of freeze-thaw cycles on properties of Integral Water Repellent Concrete*. Journal of Wuhan University of Technology-Mater. Sci. Ed., 2016. 31(4): pp. 851-856.
53. Tittarelli F. and Moriconi G., *Comparison between surface and bulk hydrophobic treatment against corrosion of galvanized reinforcing steel in concrete*. Cement and Concrete Research, 2011. 41(6): pp. 609-614.
54. Baghban M., Hovde P., and Jacobsen S., *Effect of internal hydrophobation, silica fume and w/c on compressive strength of hardened cement pastes*. World Journal of Engineering, 2012. 9(1): pp. 7-12.
55. Tittarelli F. and Moriconi G., *The effect of silane-based hydrophobic admixture on corrosion of reinforcing steel in concrete*. Cement and Concrete Research, 2008. 38(11): pp. 1354-1357.
56. SIS, *SS-EN ISO 15148 "Hygrothermal performance of building materials and products - Determination of water absorption coefficient by partial immersion"*. 2003, SIS Förlag AB: Stockholm.
57. SIS, *SS-EN 12390-3:2019 "Testing hardened concrete-Part 3: Compressive strength of test specimen"*. 2019, SIS Förlag AB: Stockholm.
58. SIS, *SS-EN 12390-1:2021 "Testing hardened concrete- Part 1: Shape, dimensions and other requirements for specimen and moulds"*. 2021, SIS Förlag AB: Stockholm.
59. SIS, *SS-EN 196-1:2016 "Methods of testing cement-Part 1: Determination of strength"*. 2016, SIS Förlag AB: Stockholm.
60. SIS, *SS 137244:2019 "Concrete testing - Hardened concrete - Scaling at freezing"*. 2019, SIS Förlag AB: Stockholm.
61. SIS, *SIS-CEN/TS 12390-9:2016 "Testing hardened concrete - Part 9: Freeze-thaw resistance with de-icing salts-Scaling"*. 2018, SIS Förlag AB: Stockholm.
62. ASTM, *ASTM C1543 "Standard Test Method for Determining the Penetration of Chloride Ion into Concrete by Ponding"*. 2010.
63. NordTest, *NT BUILD 443 "Concrete , Hardened: Accelerated Chloride Penetration"* 1995.
64. SIS, *SS-EN 12390-11:2015 "Testing hardened concrete - Part 11: Determination of the chloride resistance of concrete, unidirectional diffusion"* 2015, SIS Förlag AB: Stockholm..
65. Pedersen L., Randrup T., and Ingerslev M., *Effects of Road Distance and Protective Measures on Deicing NaCl Deposition and Soil Solution Chemistry in Planted Median Strips*. Journal of Arboriculture, 2000. 26(5).
<https://doi.org/10.48044/jauf.2000.029>
66. Lundmark A. and Olofsson B., *Chloride Deposition and Distribution in Soils Along a Deiced Highway – Assessment Using Different Methods of Measurement*. Water, air, and soil pollution, 2007. 182(1): pp. 173-185.
<https://doi.org/10.1007/s11270-006-9330-8>
67. Cement och Betonginstitutet AB, *CBI Metod Nr 5:2018, in Total klorid i hårdnad betong*. 2018, RISE AB: Stockholm.
68. Lascaray L., *Die teoretischen Grundlagen der Seifen Herstellung in Chemie und Technologie der Fette und Fettprodukte*. H. Schönfeld, Editor. 1939, Springer-Verlag Wien GmbH: Wien. p. 674.
69. Dijkstra A.J. and van Duijn G., *Vegetable Oils: Oil Production and Processing*, in *Encyclopedia of Food and Health*, B. Caballero, P.M. Finglas, and F. Toldrá, Editors. 2016, Academic Press: Oxford. pp. 373-380.
70. Hoang K., Justnes H., and Geiker M., *Early age strength increase of fly ash blended cement by a ternary hardening accelerating admixture*. Cement and Concrete Research, 2016. 81: pp. 59-69.
71. Stein H.N., *Influence of some additives on the hydration reactions of portland cement I. Non-ionic organic additives*. Journal of Applied Chemistry, 1961. 11(12): pp. 474-482.
72. Google, *Field Station Magelugnsväg*. n.d.
<https://www.google.se/maps/@59.2734392,18.0128066,3a,75y,266.47h,76.55t/data=!3m6!1e1!3m4!1sZz4cIQJzuZKpx25zHbVHvg!2e0!7i16384!8i8192>. Accessed 17th November 2022

73. Andersson L., *Continuous Preventative Bridge Maintenance; Effect of High Pressure Washing on Concrete Bridges*, Licentiate Thesis 2022, KTH Royal Institute of Technology: Stockholm.
74. Google, *Road system leading to Field station*. n.d.
<https://www.google.se/maps/@59.2733629,18.0129102,3a,75y,312.75h,90.6t/data=!3m6!1e1!3m4!1spaMIeWF4jIna8tODYTikDQ!2e0!7i16384!8i8192>
75. Svintsov A.P., Nikolenko Y.V., and Fediuk R.S., *Aggressive effect of vegetable oils and organic fatty acids on cement-sand mortar and concrete*. *Construction and Building Materials*, 2022. **329**: 127037.
<https://doi.org/10.1016/j.conbuildmat.2022.127037>
76. Garcia-Lodeiro, I., Carmona-Quiroga, P.M., Zarzuela, R., Mosquera, M.J., and Blanco-Varela, M.T., *Chemistry of the interaction between an alkoxy silane-based impregnation treatment and cementitious phases*. *Cement and Concrete Research*, 2021. **142**: 106351
<https://doi.org/10.1016/j.cemconres.2020.106351>
77. Rogers, P., Silfwerbrand, J., Gram, A. and Selander, A., *Bulk hydrophobic structural concrete for use in Nordic conditions – Initial study*. Published in: *Hydrophobe VIII*, 8th International Conference on Water Repellent Treatment and Protective Surface Technology for Building Materials, pp. 282-289, Hong Kong Polytechnic University, Hong Kong December 7th – 9th 2017
78. Rogers, P., Silfwerbrand, J., Gram, A. and Selander, A., *Bulk hydrophobic civil engineering concrete for Nordic conditions – Freeze thaw action*. Published in: *Proceedings of the fib Symposium 2019: Concrete – Innovations in Materials, Design and Structures*, pp. 2044-2051, International Federation for Structural Concrete, Krakow 27th-29th May 2019

APPENDIX 1

THIN SECTIONS OF SECOND ROUND FREEZE-THAW CONCRETES W/C = 0.40

Below are digital photographs of thin sections from all 14 concretes that were tested for F-T in 3% sodium chloride solution. These thin sections were impregnated with fluorescent epoxy, exposed to UV light and magnified to magnification x25.

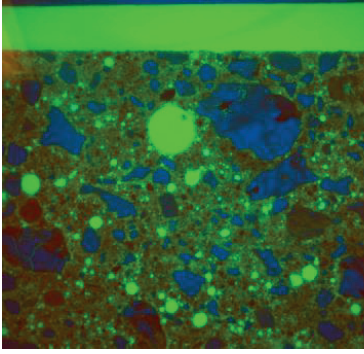
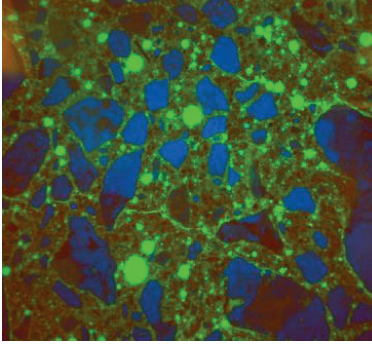
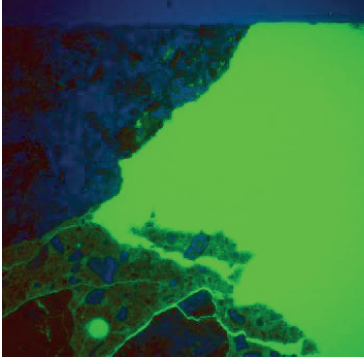
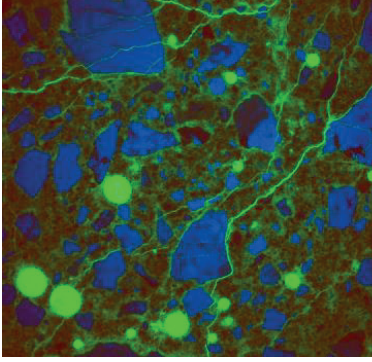
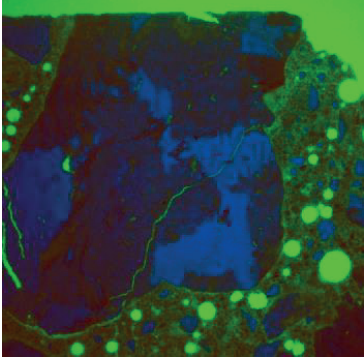
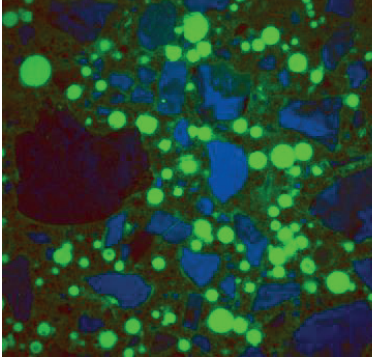
Abbreviations used in the figure explanations are :

AE = air entrainer; (X.Y%) = air content measured in fresh state, w/o = without; “+” = added.

<p>REF (0.40) w/o AE x25; Thin section; remaining surface visible (top)</p>	<p>REF (0.40) w/o AE x25; 10 mm from surface</p>
<p>REF (0.4) +AE (7.2%) x25 thin section; exposed surface (bottom)</p>	<p>REF (0.4) +AE (7.2%) x25 thin section; ca 10 mm from surface</p>

<p>REF (0.4) w/o AE (crushed agg.) x25; thin section; exposed surface (top)</p>	<p>REF (0.4) w/o AE (crushed agg.) x25 thin section; ca 10 mm from surface</p>
<p>O.O. 3% (0.40) + AE (5.4%); x25; thin section exposed surface (top)</p>	<p>O.O. 3% (0.40) + AE (5.4%), x25; thin section ca 10 mm in from surface.</p>
<p>O.O. 3% (0.40) w/o AE, x25; thin section exposed surface (top)</p>	<p>O.O. 3% (0.40) w/o AE, x25; thin section ca 10 mm in from surface.</p>

<p>R.S.O. 3% (0.40) w/o AE x25; thin section exposed surface (top)</p>	<p>R.S.O. 3% (0.40) w/o AE x25; thin section ca 10 mm in from surface.</p>
<p>R.S.O 3% (0.40) + AE x25 (6.3%); thin section exposed surface (top)</p>	<p>R.S.O 3% (0.40) + AE (6.3%) x25 thin section ca 10 mm in from surface.</p>
<p>H.X.L 1% (0.40) w/o AE x25 thin section exposed surface (top)</p>	<p>H.X.L. 1% (0.40) w/o AE x25 thin section ca 10 mm in from surface.</p>

	
<p>HMP 1% (0.40) w/o AE x25; thin section exposed surface (top)</p>	<p>HMP 1% (0.40) w/o AE x25; thin section ca 10 mm in from surface.</p>
	
<p>C.H.A 1 3% (0.40) x25 w/o AE x25; thin section exposed surface (top)</p>	<p>C.H.A. 1 3% (0.40) w/o AE x25; thin section ca 10 mm in from surface.</p>
	
<p>C.H.A 2 3% (0.40) + AE x25 thin section exposed surface (top)</p>	<p>C.H.A 2 3% (0.40) + AE x25; thin section ca 10 mm in from surface.</p>

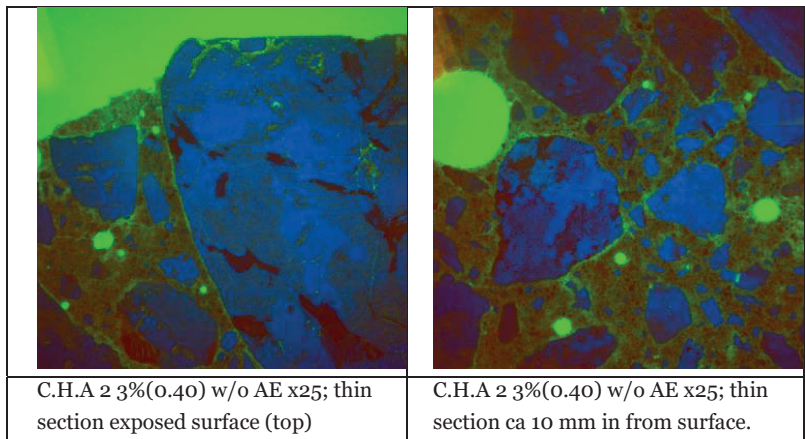
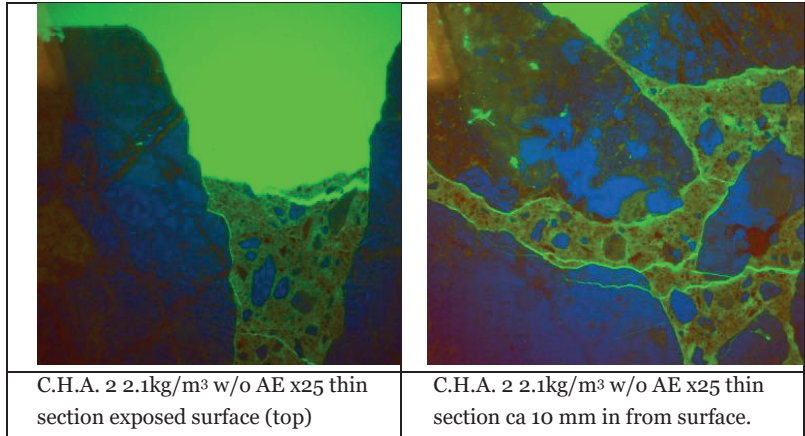


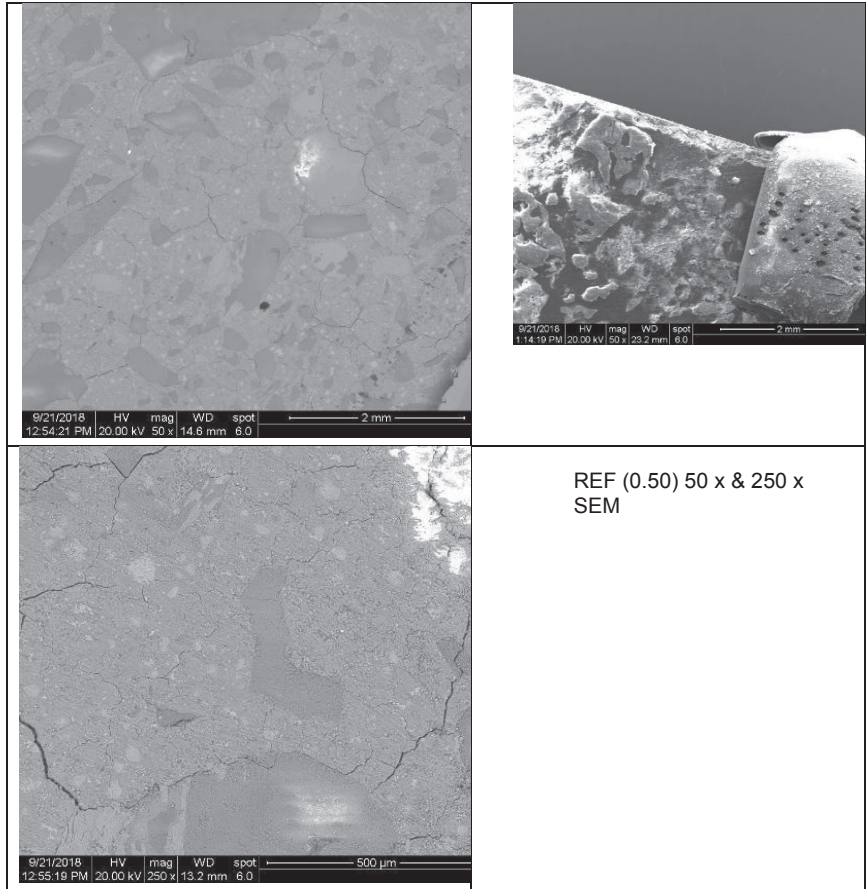


FIGURE A 2. Side profile of the top surfaces (in contact with freezing medium) of the concretes prior to thin section preparation. HXL or nr. 10 was not able to be prepared with a diamond saw and was not included in the thin section analysis. 1 = REF 0,40 w/o AE , 2 = REF = 0,40 + AE, 3 =REF 0,40 w/o AE (crushed agg), 4= O.O. 3% + AE (5.4%), 5= O.O. 3% w/o AE, 6= R.S.O. w/o AE, 7= R.S.O. + AE (6.3%), 8= H.X.L. 1% w/o AE, 9= HMP 1% w/o AE, 11 C.H.A. 1 3% w/o AE, 12 C.H.A. 2 3% +AE , 13 = C.H.A. 2 2.1kg/m3 w/o AE, 14= C.H.A. 2 3% (0.40) w/o AE.

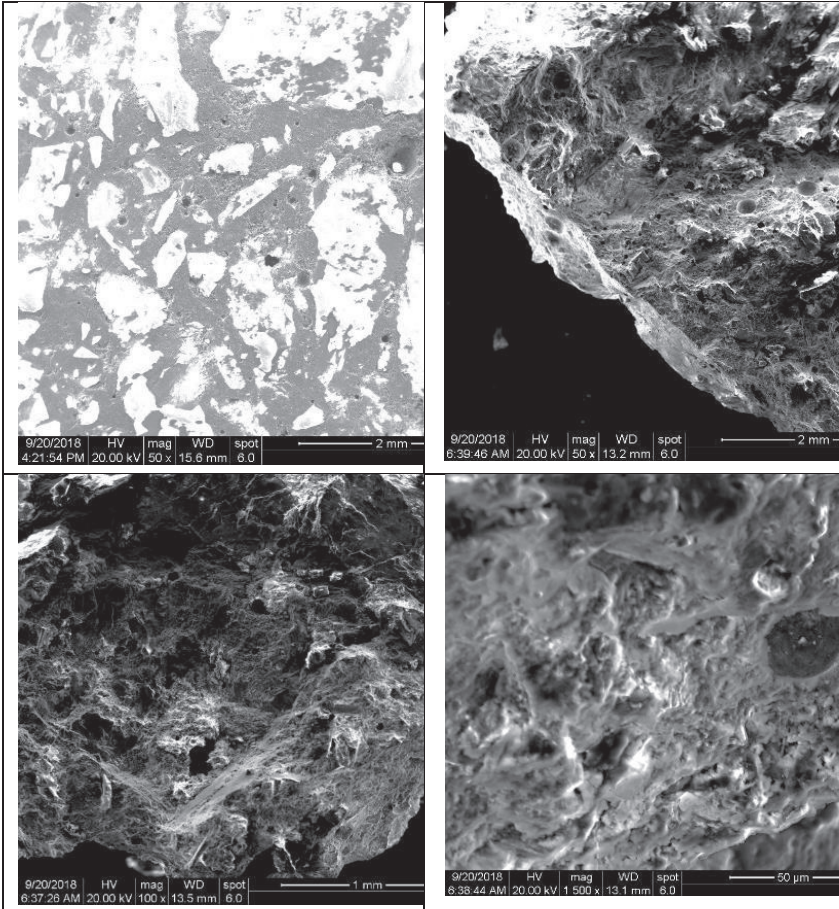
APPENDIX 2

SEM OF MORTARS FROM INITIAL STUDY, SEE PAPER 1

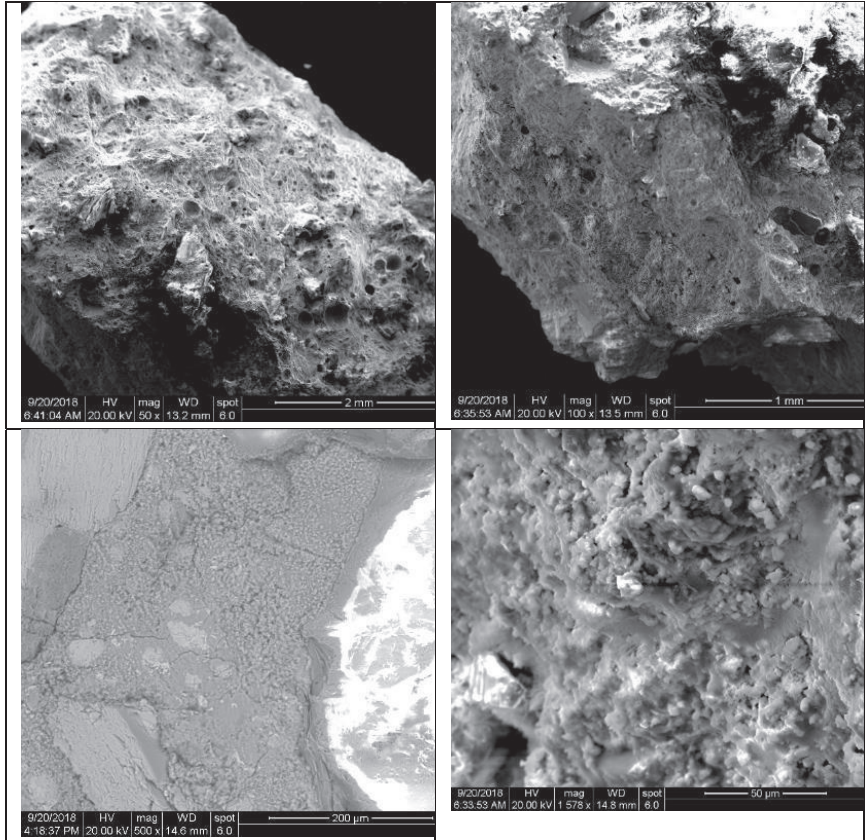
Reference Mortar (0.50)



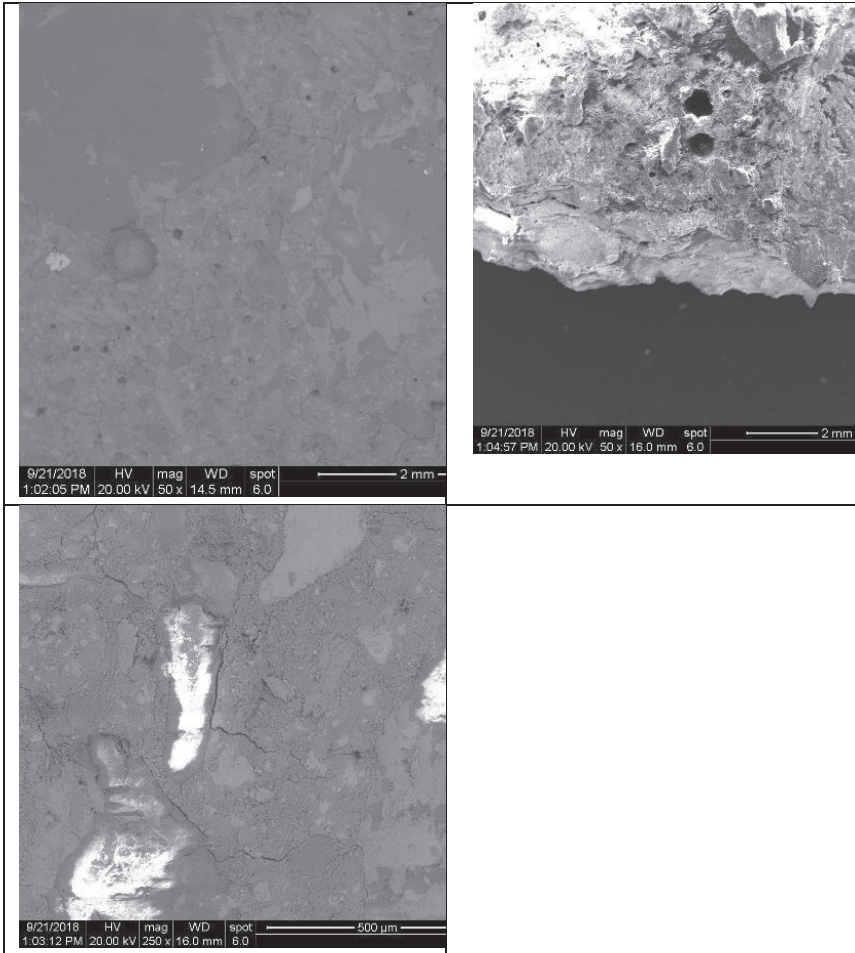
Olive Oil 3% (Mortar)



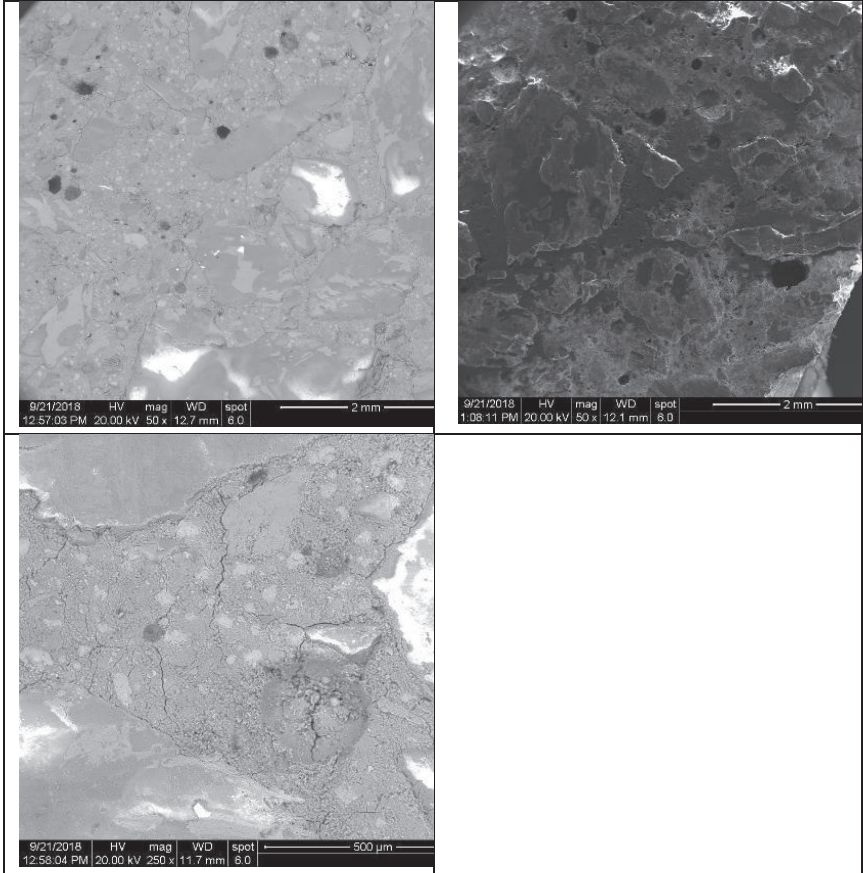
R.S.O. Mortars 3% (0.50) in mortar



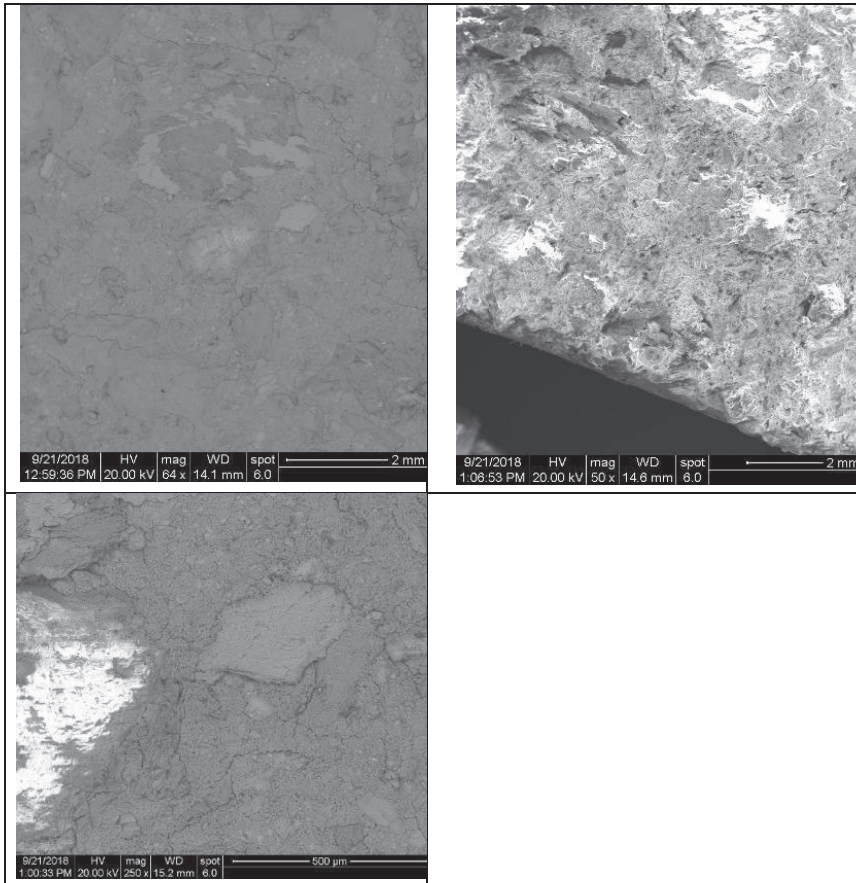
Linseed oil 3% in mortar (0.50)



Sesame seed oil 3% (0.50) in mortar



Corn Oil 3% (0.50) in mortar



APPENDIX 3

WATER ABSORPTION OF CONCRETE 20 MM THICK SPECIMENS

w/c = 0.40 with added air entrainer

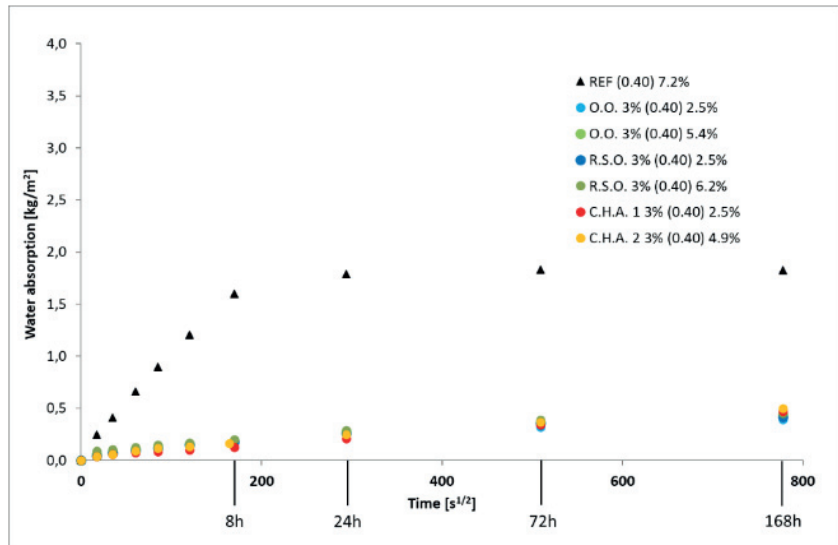


FIGURE A3.1. Water absorption of concretes (w/c = 0.40) with added air entrainer and resulting air content measurement in %.

Hydrophobic addition = 1%. Short and long term water absorption of concrete w/c = 0.50 up to 15 months.

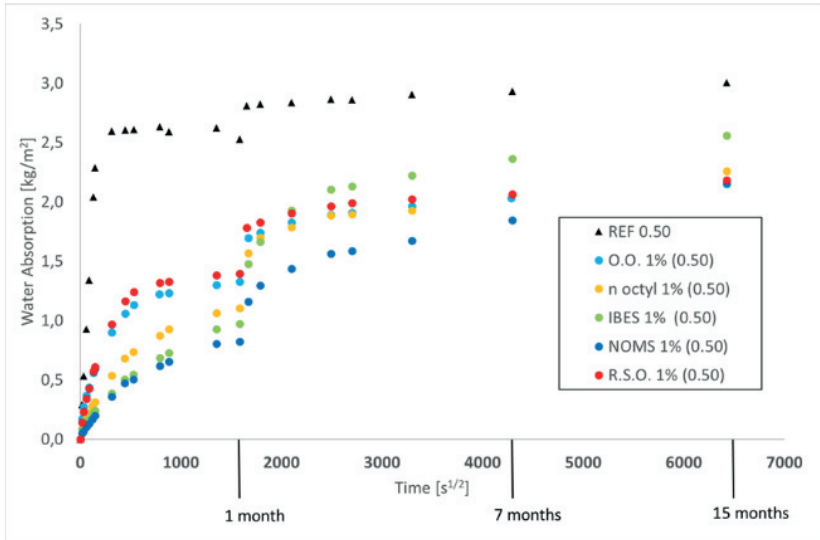


FIGURE A3.2. Long term water absorption tests w/c = 0.50 ; hydrophobic admixtures = 1%, after one month, a plastic sheet was placed over the samples. Samples = 20 mm thick.

Hydrophobic addition = 2%. Short and long term water absorption of concrete w/c = 0.50 up to 15 months.

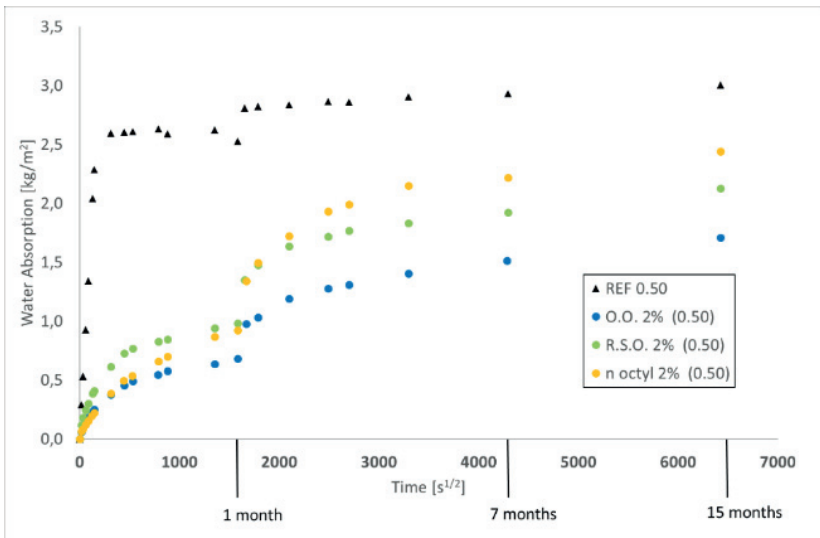


FIGURE A3.3. Long term water absorption tests w/c = 0.50 ; hydrophobic admixtures = 2%, after one month, a plastic sheet was placed over the samples. Samples = 20 mm thick.

Hydrophobic addition = 3%. Short and long term water absorption of concrete w/c = 0.50 up to 15 months.

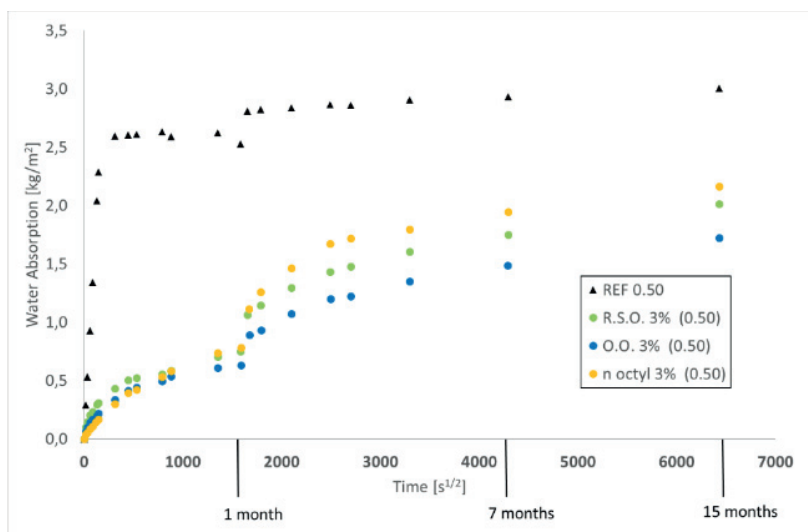


FIGURE A3.4. Long term water absorption tests w/c = 0.50 ; hydrophobic admixtures = 3%, after one month, a plastic sheet was placed over the samples. Samples = 20 mm thick.

Hydrophobic addition = 1-3%. Short and long term water absorption of concrete w/c = 0.45 up to 15 months.

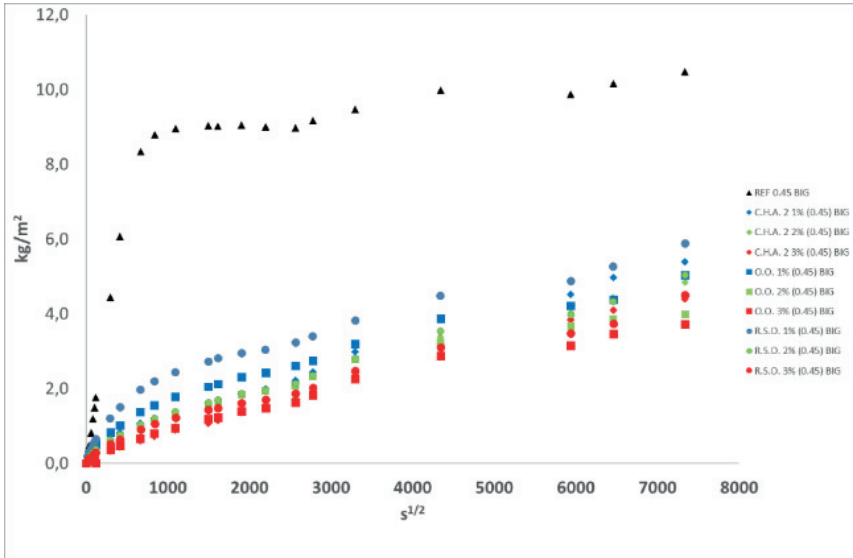


FIGURE A3.5. Long term water absorption tests w/c = 0.45 ; hydrophobic admixtures = 1-3%, after one month, a plastic sheet was placed over the samples. Samples = 80 mm thick. Red = 3% , Green = 2% , Blue = 1%, REF = Black. Circle = R.S.O, Diamond = C.H.A. 2 & Square = O.O.

APPENDIX 4

COMPRESSIVE STRENGTH

In this appendix, some of complimentary data/results are presented in regards the compressive strength including after three years.

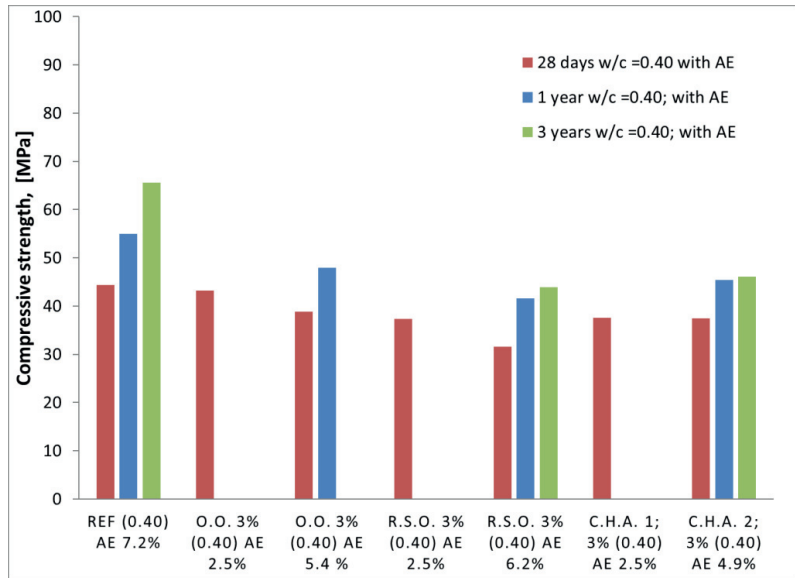


FIGURE A4.1. Compressive strengths of samples with air entrainer w/c = 0.40. Time interval 28 days, one year and three years. Not all time intervals present.

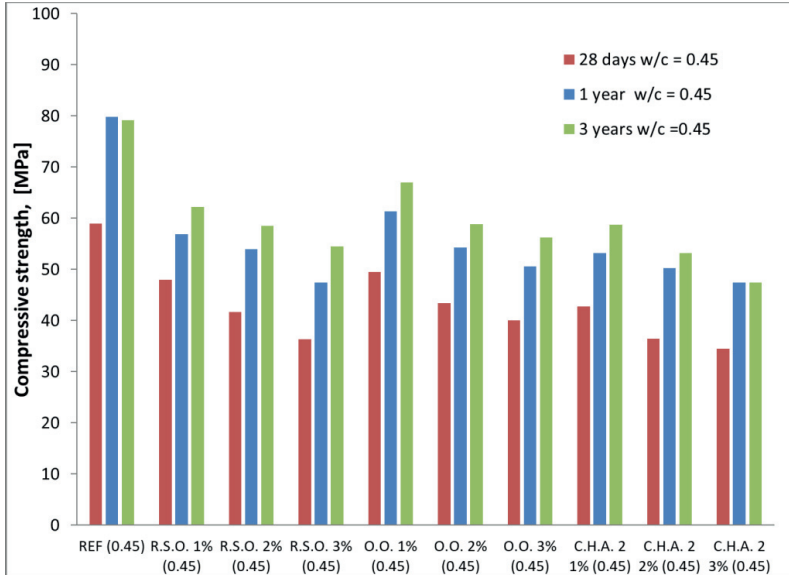


FIGURE A4.2. Compressive strength development of concretes w/c = 0.45 with varying amounts of hydrophobic admixtures (no superplasticizer nor air entrainer).

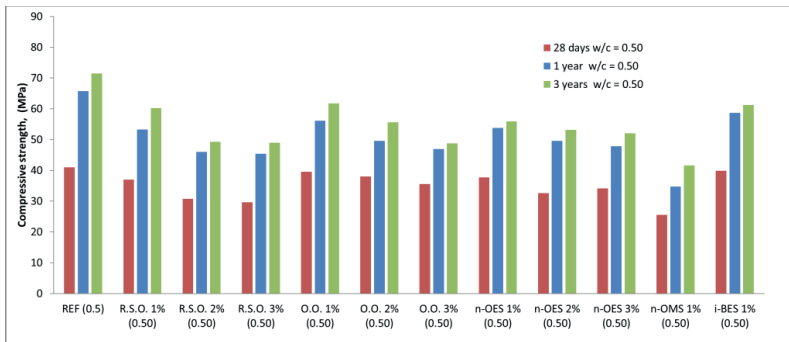


FIGURE A4.3 Compressive strength development of concretes w/c = 0.50 with varying amounts of hydrophobic admixtures (no SP or AE). 28 days = column to the left (red); 1 year = column in the middle (blue) and 3 years = column to right (green).

Increasing the amount of hydrophobic admixture in the concrete recipe decreases the compressive strength. The development of mechanical strength though is not hindered. Concrete with O.O. is generally higher compressive strengths compared to the others. The reference concrete appears to have reached a plateau. Numerically, these changes are represented

In general, the comparative difference with the reference concrete increases over time for all recipes. Within the TAGs, olive oil had the least impact on the mechanical properties of the concrete. Within the silanes, i-BES (isobutyl triethoxysilane) had the

least impact and n-OMS (n-octyl methoxysilane) had the most at comparable dosages (1%).

Compressive strengths F-T samples after 112 cycles (round 1)

Below are the compressive strength results from cored specimens from PAPER 2. These represent the average of 4 cylinders Ø50 mm.

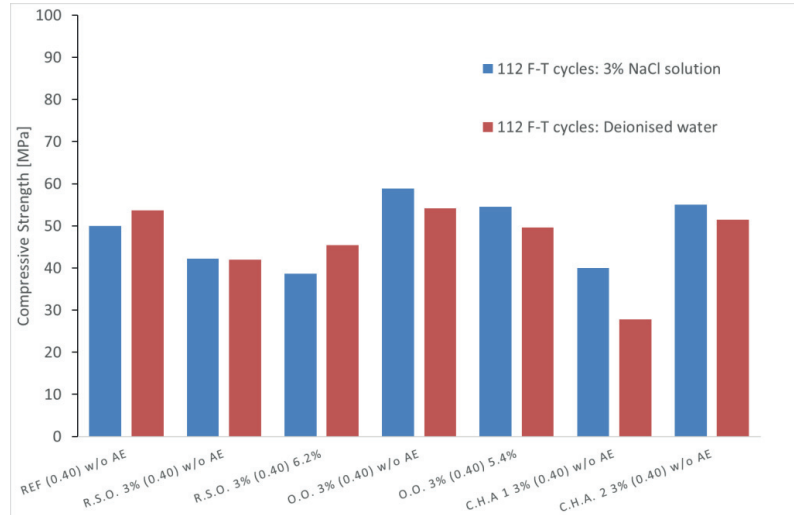


FIGURE A4.4. Compressive strengths of cylinders extracted from concrete exposed to 112 cycles in water or 3% sodium chloride solution.



FIGURE A4.5. Example of cored specimens from a concrete slab exposed to F-T testing conditions.

APPENDIX 5

ISO THERMAL CALORIMETRY

Additional data to compliment RESULTS section. Below in FIGURE A5.1 the incremental increase of unprocessed TAG (O.O) at 20 °C on cement hydration is presented.

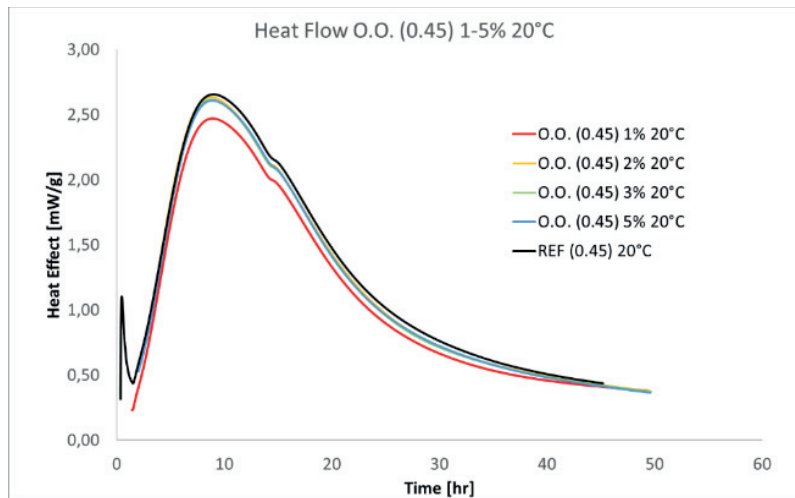


FIGURE A5.1. Results from iso calorimetry experiments of increasing unprocessed TAG (O.O) in a cement paste.

The results here show the effect of increasing the unprocessed TAG on the initial hydration of cement paste. A drop in the red line (1%) cannot be explained as the others i.e. 2,3 and 5% follow another path, very similar to the reference mix.

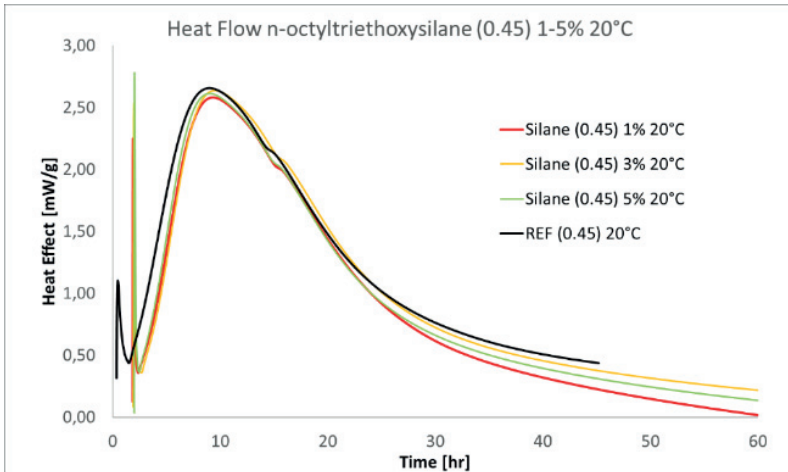


FIGURE A5.2. Results from iso calorimetry of increasing n-octylethoxysilane in a cement paste.

Results from the “Silane (0.45) 2% 20 °C” series were erroneous and were disregarded. The differences in the energy dissipated compared to the reference are insignificant. One can conclude that the addition of this particular alkyl alkosilane has no appreciable effect on the initial hydration of the cement minerals.

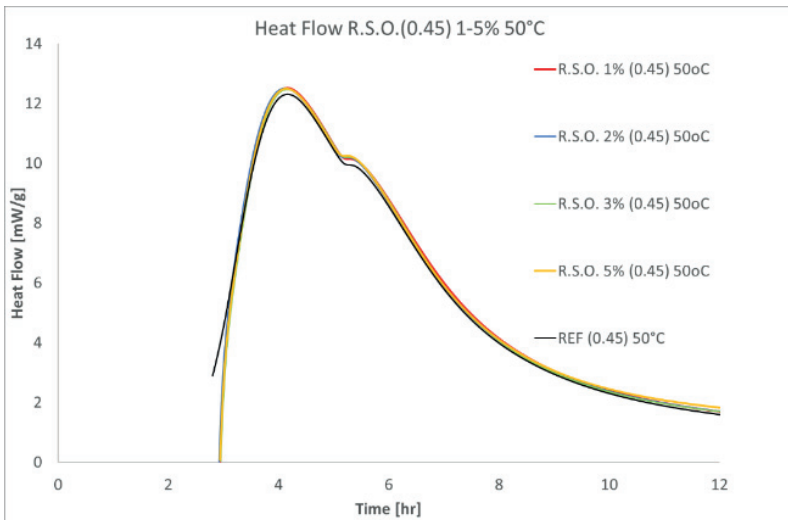


FIGURE A5.3 Results from iso calorimetry experiments using processed TAG (R.S.O.) at elevated temperature = 50 °C with adjusted REF (due to temp increase.)

In FIGURE A5.3 one sees a slight increase at 1st and 2nd heat peaks in the energy flow with the addition of processed TAG in a cement paste mix compared to the effect of the unprocessed TAG.

Complimentary experiment with “olive oil” (30% extra virgin and 70 %pomace olive oil) and also a blend of olive oil and oleic acid.

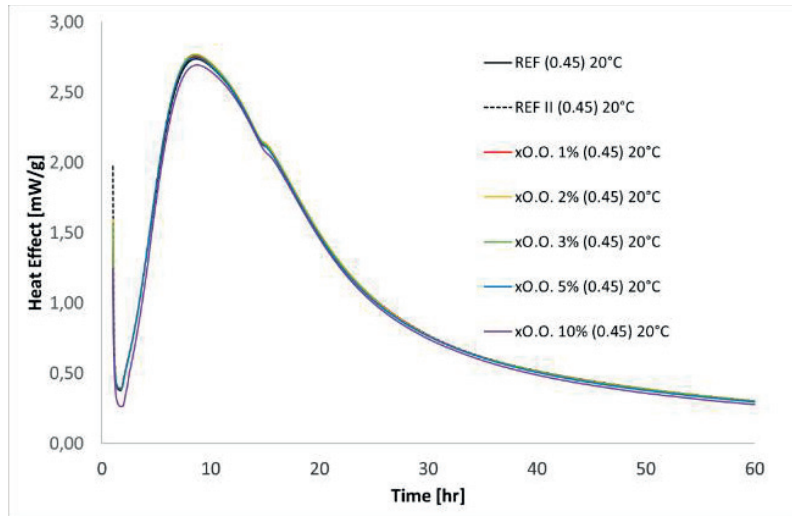


FIGURE A5.4. Results from iso calorimetry experiments using blend unprocessed & processed O.O. “olive oil” at 20 °C. Adjusted for reduction in reactive competent (CEM I). The 10% may have a dilution effect hence slightly lower (purple line)

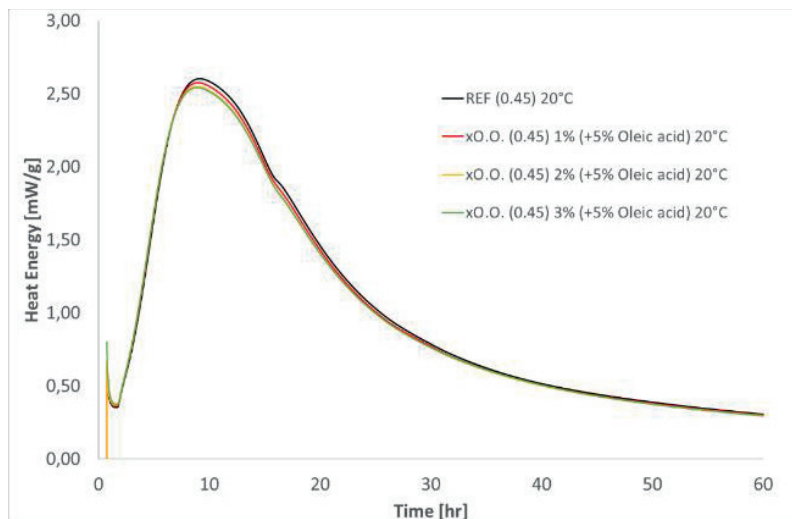


FIGURE A5.4. Results from iso calorimetry experiments using blend unprocessed & processed O.O. “olive oil” and oleic acid blended in weight ratio (95:5) at 20 °C. Adjusted for reduction in reactive competent (CEM I).

APPENDIX 6

FIELD STATION OBSERVATIONS

The field station was installed in two phases in 2018 and 2019. One operational cage, see below in FIGURE A6.1 and A6.2. All concretes are 100 mm sided sawn cubes with a 3 mm neoprene layer around the entire surface except the one facing the road.

Every year a visit is made to the field station to observe the concretes in situ, readjust the concrete specimens (if required) and to take some photos to document the appearance of the concrete, the surrounding and the cage, see FIGURES A6.1-7. No photos are available for 2022.



FIGURE A6.1. January 2018 original batch in place; REF x2 plus TAG x2 (O.O. & R.S.O) and “silane” based x2. All hydrophobic concretes dosed at 3% (based on cement weight). w/c = 0.40.



FIGURE A6.2 April 2019 installation of the longer cage with 12 recipes for this study (13-15 are from another project).



FIGURE A6.3. October 2020 original testing samples, very clean around the specimen cage.



FIGURE A6.4. October 2020 permanent marker numbering had been removed from power washing and weather.



FIGURE A6.5. October 2020 continued view of the longer cage.



FIGURE A6.6. October 2021. Original cage. No damage to the concrete surface observable.



FIGURE A6.7. October 2021. Long cage all recipes, no obvious damage to the concrete surfaces. Rust starting to form on some of the threaded parts of the cage.

50°C with oleic acid

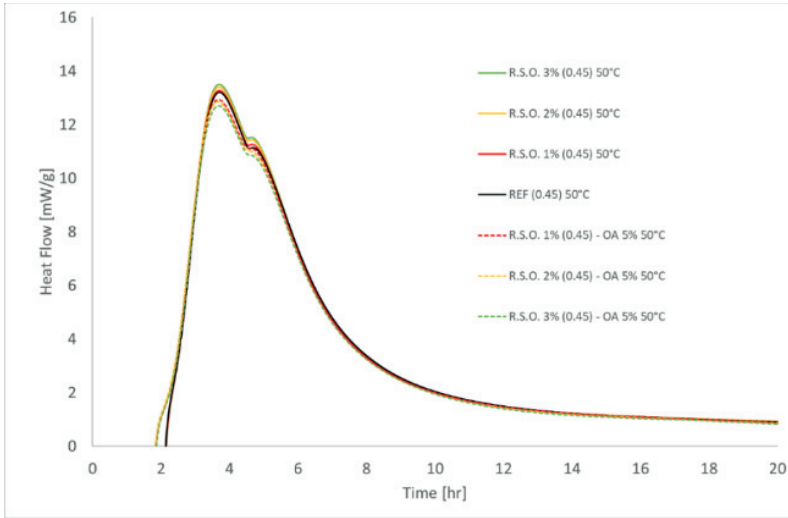


FIGURE A5.5. Iso thermal calorimetry results of R.S.O. 1-3% with and without oleic acid. The OA reduces the heat release while the cement pastes without follow the results from other observations, i.e. higher heat release with TAG (RDB).

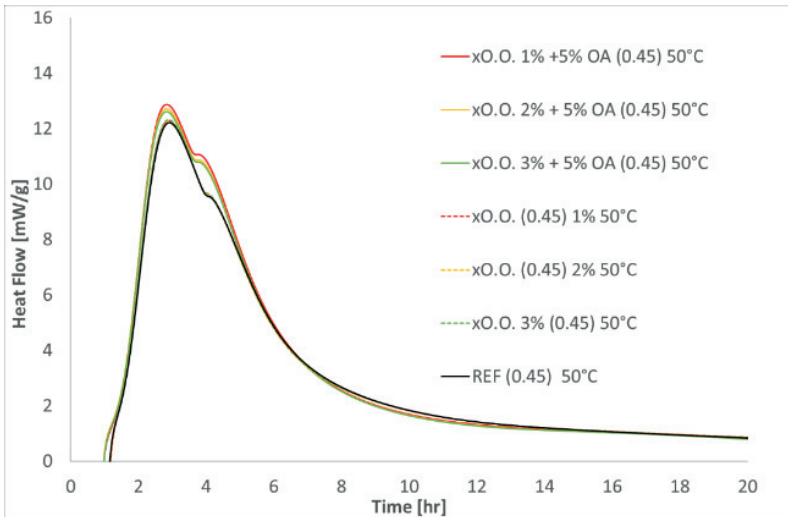


FIGURE A5.6 Iso thermal calorimetry of olive oil (1-3%) including a 5% addition of oleic acid. The addition of OA increased the release of heat energy at 1st and 2nd peak. The dotted lines follow the reference (black line)



Box 5501
SE-114 85 Stockholm

info@befonline.org • www.befonline.org
Visiting address: Storgatan 19, Stockholm

ISSN 1104-1773